University Kasdi Merbah – Ouargla

Faculty of Hydrocarbons and Renewable Energies, and Earth and Space Sciences

Department of Earth and Space Sciences

Master's Degree

Field: Earth and Space Sciences

Specialization: Petroleum Geology

Topic:

Evaluation of petrophysical parameters and study sedimentology of Zone N°23 (Hassi Messaoud region)

Presented by:
MOUISSI SABER
MEDBOUB ABDELKADER

Publicly defended on 23/06/2024

Jury:

President:	BANSIR FATEH	M.C.A. Univ. Ouargla
Supervisor	FELLAH LAHCENE	M.C.A. Univ. Ouargla
Examiner	SAHRAOUI SALAH	M.C.A. Univ. Ouargla

Academic year: 2023 / 2024

Thanks

This work would not have been possible without your support, help and encouragement.

We have continually benefited from the help of all those around us. We would like to thank them today. I would like to express my

my special gratitude:

Firstly, to Almighty God, who has given me the good will, courage and patience to accomplish this humble work.

Secondly, to Flah Lahcen for everything he has taught me and made me discover through him, and for his kindness and willingness to guide me throughout this process. We would like to tell him how enriching it is to work with him. And to all the teachers who have taught us along the way.

Finally, we would like to thank our friends who have supported us through difficult times. I would like to thank

A:

It's good to have people you can always count on.

You can always count on them

Students in the second year of the Masters in Petroleum Geology (Class of 2023_2024)

dedicate

I dedicate this humble work to my mother, who has always been the source of my happiness and support, to my father, my role model, who was waiting to see me holding my diploma, and to all my relatives and friends.

They are the reason why I reached this position and today I stand humble and proud, and I did not disappoint them.

A thousand greetings and thanks to everyone

I also do not forget the educational staff and all the honorable professors, thank you all.

Saber.M

dedicate

What could be better than being able to share the best moments of my life with those closest to me?

It is my pleasure to dedicate this humble work:

To my dear parents.

For their support throughout my school years.

To my brothers and sisters.

To all family members.

Especially all my friends from near and far.

Finally, to all my teachers from primary school to university.

In addition, thanks to

God. Peace be upon you

all.

M. Abdelkader

Abstract
Discovered in 1956, the Hassi Messaoud field in the northern Sahara Basin is one of the world's largest oilfields. Its wealth lies in a reservoir made up of thick layers of quartz sandstone dating from the Cambrian and Ordovician eras. Zone 23, the focus of this study, lies to the southwest of this oil giant. An in-depth analysis of Zone 23 was carried out using Petrel software, enabling detailed study of the deposit's petrological and physical properties, such as porosity and permeability. The results, presented in the form of isopycnal porosity and permeability maps, revealed a remarkable correlation between these properties and the quality of hydrocarbon production in the zone. The benefits of this study are considerable, including: an in-depth understanding of the characteristics of the Hassi Messaoud field, in particular zone 23; the identification of factors influencing hydrocarbon production efficiency in the study area; and valuable information for oil and gas companies operating in the area, enabling them to optimize their exploration and production processes.
Keywords: Hassi Messaoud field, Zone23, petrophysics parameters, lithostratigraphy, hydrocarbons.

ملخص
اكتُشف حقل حاسي مسعود في عام 1956، وهو أحد أكبر حقول النفط في العالم. يكمن ثراء الحقل في مكمن يتكون من طبقات سميكة من الحجر الرملي الكوارتزي الذي يعود تاريخه إلى العصرين الكمبري والأوردو فيشي. تقع المنطقة 23، وهي محور هذه الدراسة، إلى الجنوب الغربي من هذا الحقل النفطي العملاق. تم إجراء تحليل متعمق للمنطقة 23 باستخدام برنامجPétrel ، مما أتاح دراسة الخصائص البترولوجية والفيزيائية للرواسب، مثل المسامية والنفاذية بالتفصيل. كشفت النتائج، التي تم تقديمها في شكل خرائط المسامية والنفاذية المتساوية في المسامية والنفاذية، عن وجود علاقة ملحوظة بين هذه الخصائص ونوعية إنتاج الهيدروكربون في المنطقة. وقد حققت الدراسة فوائد كبيرة، بما في ذلك: فهم متعمق لخصائص حقل حاسي مسعود، ولا سيما المنطقة 23؛ وتحديد العوامل التي تؤثر على كفاءة إنتاج الهيدروكربون في المنطقة المدروسة؛ وأخيراً، معلومات قيمة لشركات النفط والغاز العاملة في المنطقة، مما يمكنها من تحسين عمليات التنقيب والإنتاج.
الكلمات المفتاحية: حقل حاسي مسعود، المنطقة 23، بارامترات الفيزياء البترولية، علم طبقات الأرض، الهيدروكربونات.

Résumé
Découvert en 1956, le gisement de Hassi Messaoud, niché dans le nord du bassin du Sahara, s'impose comme l'un des plus vastes champs pétrolifères au monde. Sa richesse réside dans un réservoir constitué d'épaisses couches de grès quartzique datant des ères Cambrienne et Ordovicienne. La zone 23, au cœur de cette étude, s'étend au sud-ouest de ce géant pétrolier. Une analyse approfondie de la zone 23 a été menée à l'aide du logiciel Pétrel, permettant d'étudier en détail les propriétés pétrologiques et physiques du gisement, telles que la porosité et la perméabilité. Les résultats, présentés sous forme de cartes de porosité et de perméabilité isopycnal, ont révélé une corrélation remarquable entre ces propriétés et la qualité de la production d'hydrocarbures dans la zone. Cette étude a apporté des avantages considérables, notamment : Une compréhension approfondie des caractéristiques du champ de Hassi Messaoud, en particulier de la zone 23, l'identification des facteurs influençant l'efficacité de la production d'hydrocarbures dans la zone étudiée, et enfin des informations précieuses pour les compagnies pétrolières et gazières opérant dans la zone, leur permettant d'optimiser leurs processus d'exploration et de production.
Mots-clés : Champ de Hassi Messaoud, Zone23, paramètres pétro physiques, litho stratigraphie, hydrocarbures.

INTREDUCTION

Chapter I: Generality

Chapter II Used Methods and materials

List figure

Symbols and abbreviations

DP: division production.

SH: SONATRACH

HMD: Hassi Messaoud

P: Pression

Q: Debit

D3: Medium fine

D4: Upper Coarse

Id: internal exchange.

PHI ϕ: Porosity

K: permeability

SW: saturation

Id: internal exchange

D3: Medium fine

MD: Wells

General introduction

Introduction

Geology of the Hassi Messaoud Oil Field: Located in the heart of the Algerian desert, 800 km south of the capital Algiers, the Hassi Messaoud field is one of the most important oil fields not only in Algeria but in the world.

Giant oil wells adorn the Hassi Messaoud plain, like a masterpiece painted by the hand of nature. Every year, these wells pump huge quantities of black oil, replenishing the coffers of the Algerian state and contributing to economic development.

The Hassi Messaoud oil field is located in Algeria's Ouled Jarara Basin and is the country's largest oil field The field is characterized by its complex geological formation, which comprises a variety of sedimentary layers formed during different time periods.

Main layer:

- **Jurassic layer:** This layer consists of limestone and sand and is rich in organic matter that has been converted into oil and gas.
- **Cretaceous:** This layer consists of chalk and limestone and is an impermeable cap that prevents oil and gas from seeping into the surface layers.
- **Paleogene:** This layer consists of clay and sand and is an important reservoir layer where large quantities of oil and gas accumulate.
- **Neogene:** This layer consists of clay and sand and is an impermeable layer that prevents oil and gas from escaping to the surface.

Geological Structures:

The Hassi Messaoud field is characterized by the presence of several geological structures that play an important role in the distribution of oil and gas reserves, the most important of which are:

- **Salt dome:** It is a dome-shaped geological structure composed of rock salt, and this dome has played an important role in trapping oil and gas in the Paleogene layers.
- **Faults:** These are fractures in the earth's crust that have contributed to the formation of oil and gas traps.

Factors affecting the distribution of oil and gas reserves:

- **Rock type:** Oil and gas reserves are concentrated in sedimentary layers with high porosity and permeability, such as limestone and sand.
- **Geological structures:** Geological structures, such as salt domes and fissures, play an important role in confining oil and gas to specific locations.
- **Depth of strata:** The amount of oil and gas increases as the depth of the sedimentary layers increases.

Importance of the Hassi Messaoud field:

The Hassi Messaoud field is one of the most important oil fields in the world, playing an important role in meeting Algeria's energy needs. It also contributes significantly to the national economy through export revenues.

The problem

Area 23, located southwest of the Hassi Messaoud field, contains hydrocarbons, but we do not know the amount °°°of its production? Therefore, we will study its petrophysical characteristics.

Chapter I

generality

1. Field history:

The Hassi Messaoud deposit was discovered on January 16, 1956 through the first MD1 drilling; It was planted after conducting a refractive seismic survey near Bir El Camel in Hassi Messaoud On June 15 of the same year, this drilling discovered oil in Cambrian sandstone at a depth of 3,338 meters[1].

Therefore, the deposit is covered by two distinct privileges:

- In the north C.F.P.A.
- To the south SN. REPAL

The boundary cuts the field in the east-west direction into two approximately equal parts.

2. Geographical location:

The Hassi Messaoud field is located 650 km southeast of Algiers and 350 km from the Tunisian border. The field dimensions reach 2,500 km2 and an oil-impregnated area of about 1,600 km2. Its location[1]:

The coordinates of the Lambert region in southern Algeria are as follows:

- 790.000 840.000 EAST
- 110.000 150.000 North

3. In geographical coordinates:

- North latitude 32 15 ° - West longitude 5 40°
- South latitude 31 ° 30 - East longitude 6 35 °

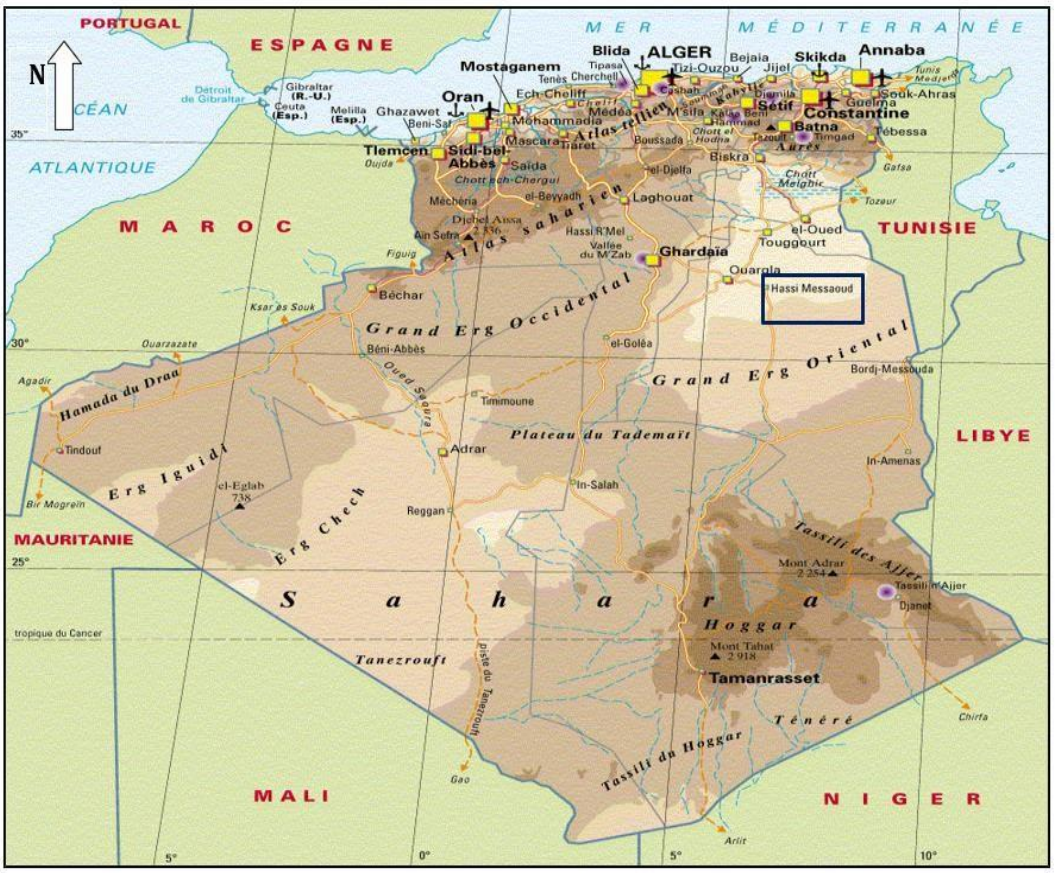

Fig.I.1. Geographical location of the Hassi Messaoud field[2]

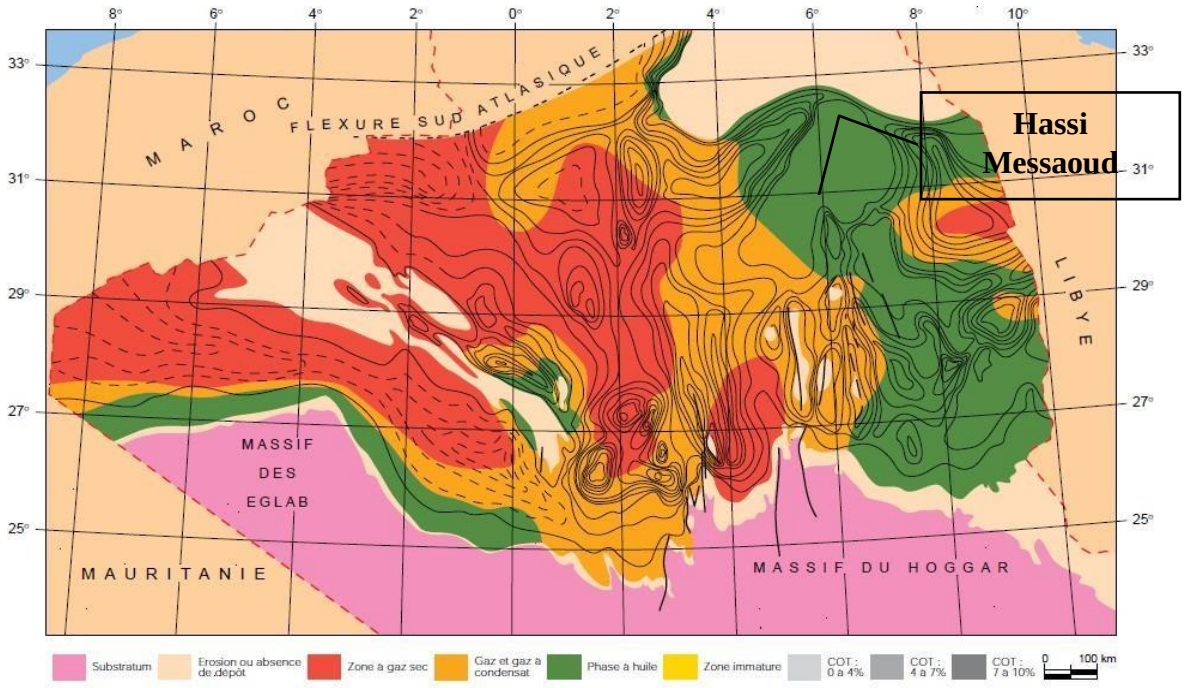

Fig.I.2. Geological context of the Hassi Messaoud field (In Sonatrach, 2005)[3].

4. Geological situation:

The Hassi Messaoud field occupies the central part of the Triassic region, east of the Oued Mia depression in the fourth region, which is considered, in terms of its surface area and reserves, the largest oil and gas region. It is the largest warehouse in Algeria, extending over an area of 53 x 44 km[1].

It is limited:

- In the northwest of the Ouargla deposits [Guelala, Ben Kahla and the Berkaoui basin]
- To the southwest of the deposit El Gassi, Zotti et El Agreb.
- To the southeast of the deposit; Rhourde El Baguel et Mesdar.

More broadly, they are geologically limited:

- To the west of the depression by Oued Mya.
- To South in Mole by Amguid El Biod.
- To the north of the structure Djammâa-Touggourt.
- To the east are the Dahr shoals, Rhourde El Baguel and the Birken depression.

5. Field structure:

The structure of Hassi Messaoud develops into a broad semi-circular anticline with a diameter of 45 km, direction: north-east/southwest. It is partially cracked and these cracks are due to plate tectonic movements that caused the structure to tilt.

The Accidents affecting the reservoir are of two types:

- Sub-meridional trend faults and other perpendicular faults in the northwest/southeast direction, which highlights the tectonic character.

- Separators without releases, which have a significant impact on fracturing the reservoir

Dry wells are generally associated with tectonic events and associated fractures.

From the characteristic point of view of the reservoir, the Hassi Messaoud deposits are defined in an ideal triplet:

- Heterogeneous: both vertically and horizontally.
- Intermittent: with fluid flow.
- Anisotropic: in the presence of silt.

6. Field division:

The Hassi Messaoud field remains traditionally divided into Hassi Messaoud to the north and Hassi Messaoud to the south[4].

The field is currently divided into 25 production areas. These areas are relatively independent and correspond to a group of wells that communicate with each other lithological and behave in the same way from the pressure point of view.

The Hassi Messaoud field is divided from east to west into two distinct parts: north and south, each with its own numbering[4].

7. Description of the reservoir:

The Hassi Messaoud deposits are characterized, as mentioned above, by their Cambro-Ordovician reservoir. Its depth ranges between 3100 and 3380 m. Its thickness reaches 200 m. Its oil has an API grade of 45.4, and its initial pressure rose to 482 kg/cm2 for a bubble point between 140 kg/cm2 and 200 kg/cm2. The HMD field is part of the eastern region of the desert platform. This governorate contains the main accumulations of hydrocarbons in the desert.

In Hassi Messaoud, hydrocarbons are located in the Cambro Ordovician region, which is divided from bottom to top into:

- Sandstone from Hassi Messaoud.
- Sandstone from EL- GASSI The lower part of the sandstone clay in Wadi Mia. The Hercynian unconformity has eroded much of the Paleolithic terminology, so it is the Triassic that forms the reservoir cap

7.1. Geology of the Hassi-Messaoud reservoir:

➢ The Cambrian:

It is represented by heterogeneous levels of fine to coarse sandstone, intersected with siliceous clay-mica layers, and these materials are called Masoud sandstone.

From bottom to top, the Cambrian reservoir is divided into four lithology levels R3, R2, Ra for the Hassi Messaoud sandstones and Ri for the Hassi Messaoud sandstones and sandstones from El- Gassi.[4]

A. Level R3*:*

It is characterized by the following:

- Maximum non-corroded thickness of 270 m
- Sand, gravel and other minerals such as feldspar, mica and siderite.
- 30% clay (élite and kaolinite) on average.
- -It's very impermeable.
- Water saturation is always taken into account in 70 to 80% of the areas of the HMD field.

B. Level R2:

It is divided into two sub-levels:

As for the **R2C** and **R2AB** levels, the **R2** level is characterized by the following:

- Average uncorroded thickness of 80 m.
- Grains with improved sphericity.
- 17% clay on average.
- Improved permeability in **R2AB**.
- Its water saturation is always taken into account.

C. level Ra*:*

It is characterized by the following:

- Average thickness is 120 m.
- A decimeter-thick sedimentary unit with inclined layers, organised into a metric-thick gutter-shaped sedimentary structure.
- Grains are somewhat spherical, poorly sorted.
- From 5 to 15% clay (illite, especially kaolinite).
- The strata consist of a succession of well-sorted coarse sand deposits with low clay content and more or less fine sediments and classified with intermittent clay (silt) intrusions.
- Compacting the sediment, dissolving and then precipitating the silica reduced the permeability and porosity to their present value.

The Ra River, in turn, is divided into three sedimentary regions.

1. **Region1:**

   The bottom total is divided from bottom to top by:

   - Drain D1.
   - Exchange ID (internal exchange).
   - Drain D2.

2. **Region 2:**

   - Medium fine or also Drain D3.

3. **Region3:**

   - Upper Coarse or Drain D4.

D. Levels Ri (5):

It is characterized by the following:

- Average uncorroded thickness 45m (in non-corroded condition)

It is deposited on Ra and sometimes directly on D3 when D4 is not deposited, as in the East and Southeast of the field.

This composition is:

- About 30% clay.
- Reduced grain size.
- Good continuity of layers.
- Low permeability.
- Sandstone pressure.

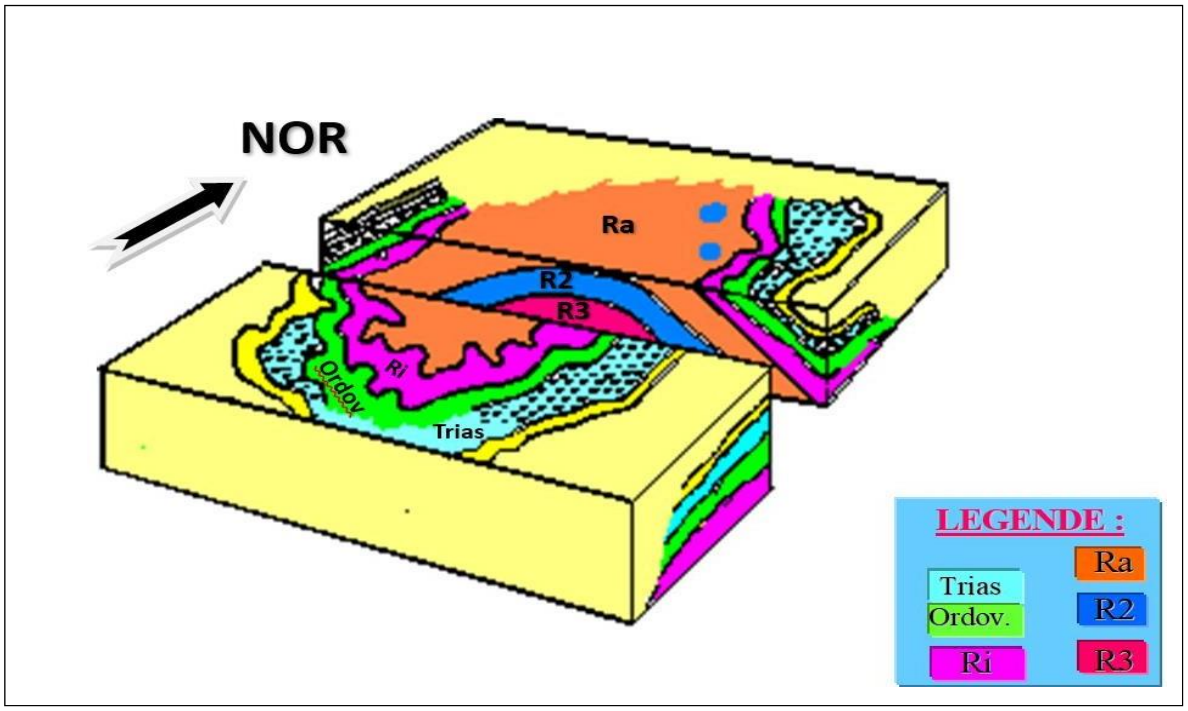

Fig.I.3. DEPOSIT OF HASSI MESSAOUD BLOCK DIAGRAM OF THE GEOLOGICAL FLOOR BENEATH THE HERCYNIAN DISCORD

8. Average petrophysical characteristics of the Cambrian reservoir:

Reservoir	K min (md)	K moy (md)	K Max (md)	Φmin %	Φmoy %	Φmax %	Swi %
Ri	**0.3**	**1**	**2**	**6**	**7**	**8**	**17**
Ra	**2**	**15**	**100**	**6**	**8**	**10**	**10**
R2	**1**	**2.5**	**7**	**-**	**10**	**-**	**17**

9. Average thickness of drains:

Reservoir	Drains	thickness(m)		
Ri	**D5**	**40**	**45**	**50**
Ra	**D4**	**25**	**32**	**40**
	D3	**18**	**22**	**26**
	D2	**20**	**24**	**30**
	ID	**25**	**28**	**32**
	D1	**27**	**30**	**33**
R2	**R2ab**	**33**	**35**	**38**

10. Origin of the oil:

The Hassi Messaoud reservoir is located at an average depth of 3,350 meters in Cambrian quartz terrain.[5, 6]

According to the Cambrian dating of Hassi Messaoud by the Mobile Field Research Laboratory, there are two possible sources of origin for the oil:

- Clay banks of gassy clay due to their presence near the field, especially the advanced state of carbonation, which attests to their contribution to the hydrocarbon formation process.
- Silurian clay, which is a strong series rich in organic materials located on both sides of the sediments, and has great depths.

Depending on geochemical tests, these clays represent the potential major source rocks that produced much of Hassi Messaoud's oil.

The oils formed from the beginning of the Jurassic migrated to the Lower Cretaceous, where they were trapped.

10.1. Properties of fluids:

The oil has different properties depending on the region. In the East, the bubble point can reach 200 g\cm for a gas/oil melting ratio of 240 cm3/m3. In the West, it can decrease to 140 kg/cm2, with an oil/gas melting ratio equal to 160 cm3/m3.

Below are the average fluid properties provided for Hassi Messaoud.[2]

A- Properties of oils: the following

- Light oil with density of 0.8 (API = 45.4)
- Tank pressure is variable: 400 to 120 kg/cm2.
- The temperature is about 118 degrees Celsius.
- GOR is 219 m3/m3 except for penetration wells where GOR can reach 800 m3/m3 and more: OML cases 63 and 633)
- Low average porosity: 5 to 10%.
- Permeability is very low.
- Viscosity 0.2 cp.
- The scale factor is 1.7.

11.Operational problems facing the Hassi-Messaoud field:

The Hassi Messaoud field presents production problems that are generally exacerbated by the extreme temperature and pressure conditions prevailing in the deposits.

The first problem is due to asphalt deposits in the pipes.

The second is due to the presence of saturated salt water in the bottom conditions during formation. These deposits cause blockages and significantly reduce the productivity of wells.

The presence of salt water in the formation causes salt crystals to precipitate in the pipes once quantities of water, even very small, are produced with the oil. It is the result of a change in thermodynamic conditions. To prevent these salt deposits, continuous fresh water injection or caps are recommended.

Since the injected water is not compatible with the tank water, new deposits (barium sulfate) occur in the pipes. These barium sulfate deposits are very difficult to remove despite the injection of a deposit inhibitor[2].

Penetration of gas and water into producing wells in the injection area poses production problems. The latter significantly reduces the productivity index, especially in water penetration wells. These wells require short-term gas lift to maintain their production, and thus additional investments.

Gas breakthroughs are less dramatic but require wells to be operated at high pressures and cause additional pressure losses during assembly.

12.Average petrophysical characteristics of the Cambrian reservoir:

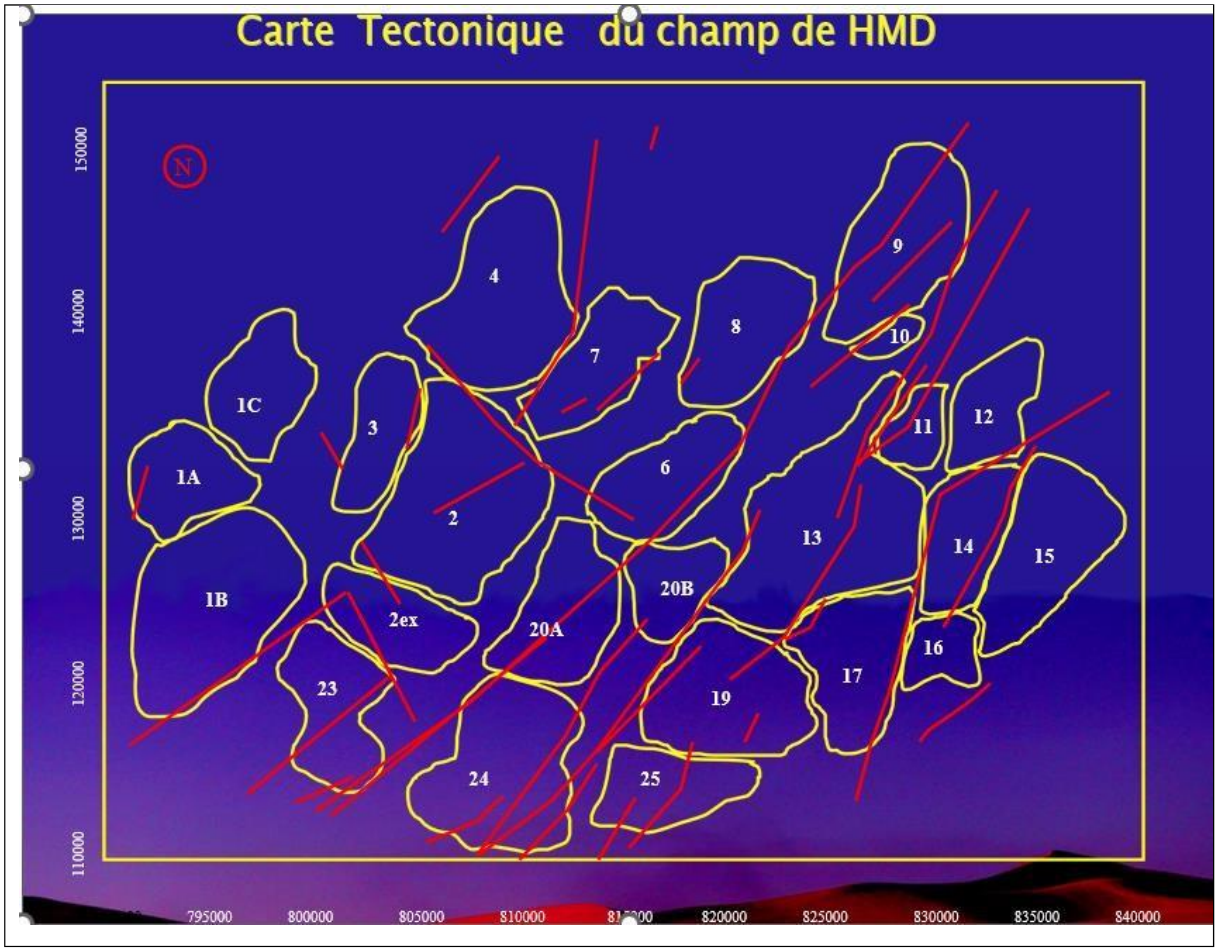

Fig.I.4. Division of Hassi Messaoud field (Document: Sonatrach DP-HMD, geological department, study service

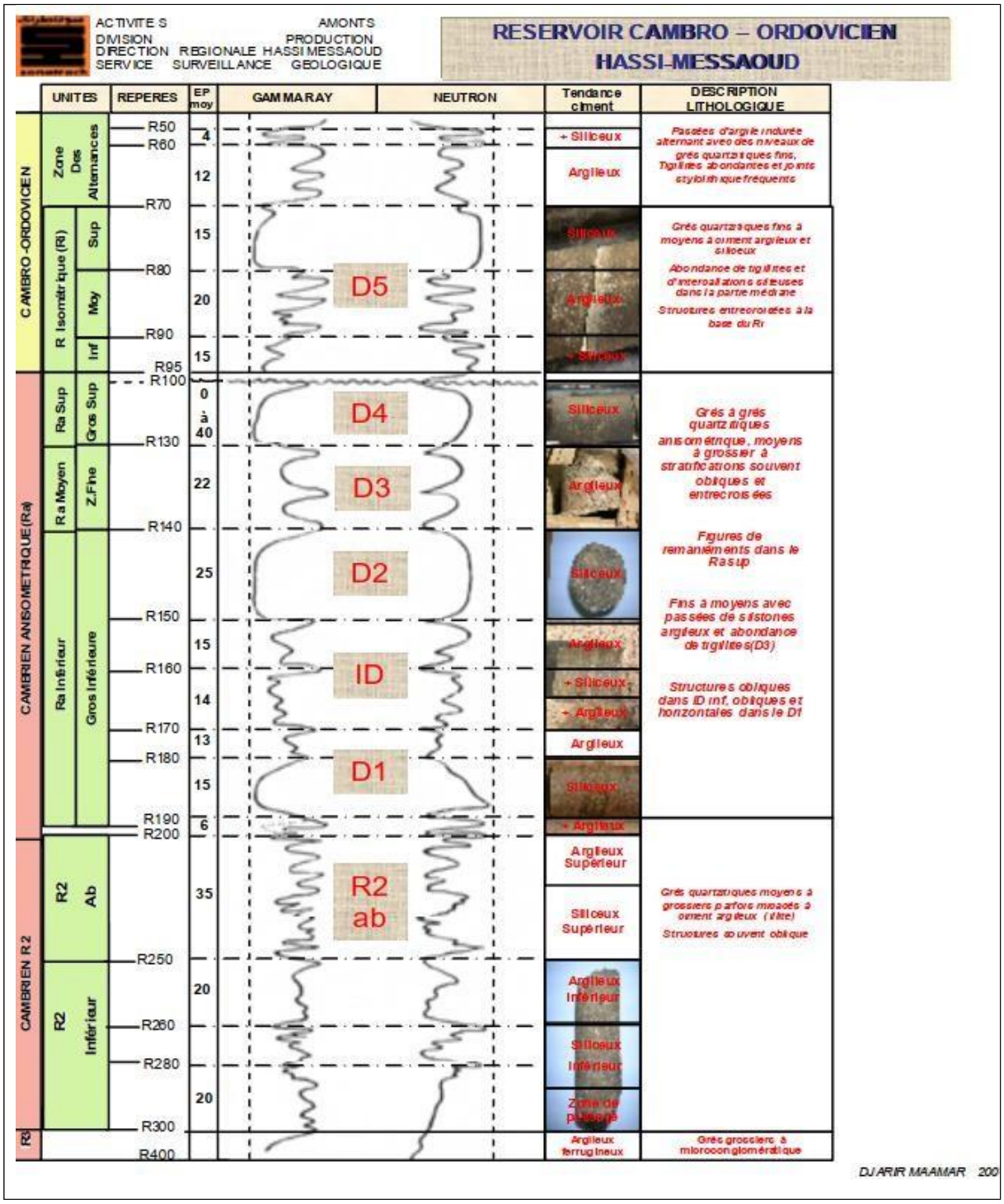

Fig.I.05. Typical Cambro-Ordovician stratigraphic section of the Hassi-Messaoud field[5]

Chapter II:

Used Methods and materials

1. Introduction:

The strategy followed in this study was to carry out a static characterization using geological data, starting with the acquisition and processing of raw data;

Loading of the data; structural modelling and modelling of the properties; this modelling is based on the Petrel software; in our case, we chose Zone23.

2. Concept and objective:

The concept of modelling is to create a representation of the subsurface of a rock formation in the form of a 3-dimensional grid of small parallelepipeds (blocks) ranging in size from a few meters to a few tens of meters, all of the same size hence the name block model.

The main objectives of the modelling are to:

- Characteristics the various petrophysical parameters using core and log data.
- Draw up maps (isobaths, iso-porosity, iso-permeability, is opaque, iso-argyle site).
- Establish patio-temporal correlations between the different wells considered.
- Propose a 3D geological model of the reservoir studied.
- Estimate the field's capacity and look for optimum locations for the production wells.
- See how the field develops over the medium and long term.
- The models can be updated immediately as new data comes in, so decisions can be made faster and more accurately to make faster, decisions that are more reliable.

3. Method used in geological modelling:

Mathematics applied to geology has given rise to a new discipline, “Geostatistics”, on which reservoir modelling is based. Geostatistics is a discipline at the frontier between mathematicsand the earth sciences. It is a static evaluation of reservoirs, making it possible to process a set of spatially distributed data in a given area in order to estimate the values in its vicinity based on a set of samples taken at different locations, which in turn are taken as references.

Pixel-based method:

This method utilizes kriging (an estimation method derived from Geostatistics) and therefore requires the definition of a variance plot (a mathematical function that expresses the evaluation of the sampling measurement variance as a function of the distance between each pair of samples). The value to be simulated at a given node is independently correlated with

each neighboring value. These methods are not suitable for channel simulation, as they cannot reproduce the curved and continuous shape of river sediments. These methods are not suitable for channel simulation, as they cannot reproduce the curvilinear and continuous shape of fluvial deposits:

4. Sequential Indicator Simulation:

This algorithm is commonly used for modelling geological facies, rock types, where there are a number of trends that can change. Its output will depend mainly on:

The scaling of the recorded data.

5. Presentation of PETREL software:

In recent years, integrated workstations have made their appearance in the oil industry, thanks to the real development of microelectronics and computing.

These machines make it possible to carry out a number of tasks in the various fields of oil exploration, in particular the interpretation of 3D or 2D seismic data, simplifying and automating many of the geologist's and geophysicist's tasks.

To this end, the SCHLUMBERGER petroleum services company has developed a high-performance Windows-based software package, PETREL, for 3D visualization, 3D mapping and reservoir modelling and simulation.

- The values that define the variogrammes.
- Frequency of distribution of log data.

This algorithm has been designed for discrete data (data whose values are represented by real numbers.) The mechanism is similar to a sequential Gaussian simulator with a few exceptions.

This method is used to calculate the lithology and facies grids.

5.1. Description of PETREL software

Development on the Petrel software began in 1996 in an attempt to combat the problems of specialist geophysicists. The result was an integrated workflow tool that allows companies to think creatively about their reservoir and allows specialist geologists and geophysicists to

work together with the tools available. The Petrel software is now a complete simulation application.

The user interface is based on Microsoft Windows standards of buttons, dialogues and help systems. This allows the majority of users to become familiar with the application and ensures that it is used effectively.

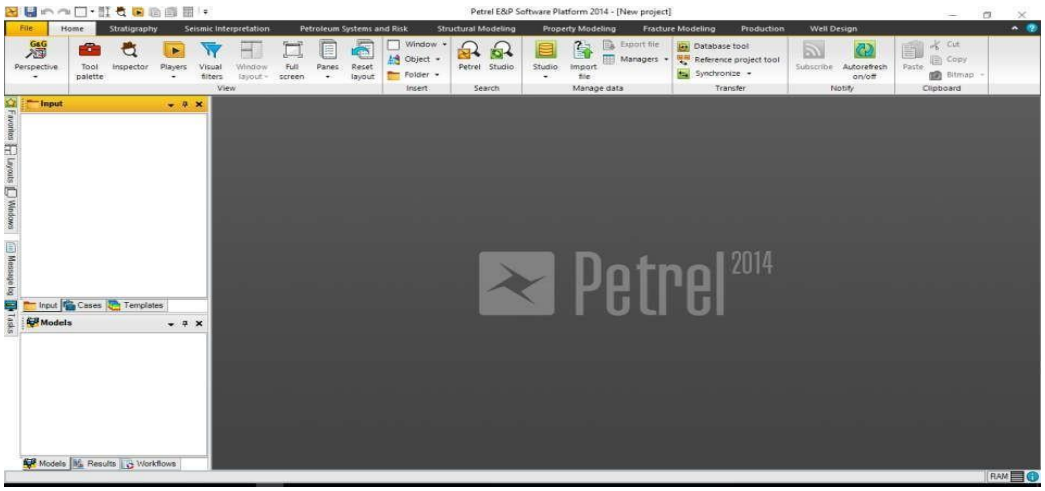

Fig.II.1.the petrel 2014 software interface

6. Origin Pro:

Origin Pro is advanced computer software for data analysis and visualization. It is widely used by researchers, engineers and scientists in a variety of fields including physics, chemistry, biology, engineering and medicine. Origin Pro provides a wide range of tools for analyzing data and creating high-quality graphs, as well as powerful image processing and signal analysis capabilities.

6.1. Origin Pro features:

- Data Analysis

Origin Pro provides a wide range of data analysis tools including basic statistics, regression analysis, spectral analysis and experimental design analysis.

- Visualization Origin Pro can create a wide range of 2D and 3D graphs, including pie, line, bar, surface and polar plots.

- Image processing Origin Pro provides tools for image processing, including noise reduction, image filtering, and image analysis.
- Signal Analysis Origin Pro can analyze signals, including Fourier transform, wavelet analysis, and filter analysis.
- Programming Origin Pro supports a built-in programming language called Lab Talk, which allows users to create custom analysis and visualization tools.

6.2. User Interface Explained:

The Origin Pro user interface consists of the following windows:

- Project Window: This window is used to view currently open projects.
- Data Window: This window is used to view and analyze data.
- Graph Window: Use this window to create and edit graphs.
- Dashboard window: Used to view and visualize data analysis options.
- Command Line Window: This window is used to enter Lab Talk commands.

6.3. How to use Origin Pro:

For basic use of Origin Pro, follow these steps:

- Import data Import your data from a file or enter it manually.
- Analyze the data Select the type of analysis you want to perform and apply it to your data.
- Create a graph Select the type of graph you want to create and create it from your data.
- Customize the graph Customize the appearance of the graph to make it look the way you want.

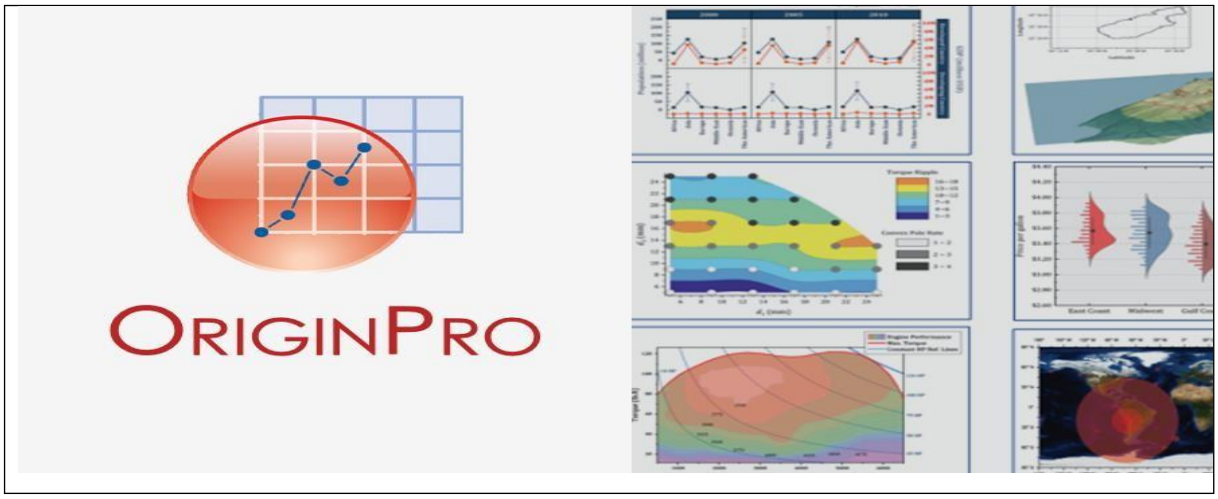

Fig.II.2. Origin pro software

7. Statistica:

Statistica is advanced computer software for data analysis and visualization. It is widely used by researchers, engineers and scientists in various fields, including physics, chemistry, biology, engineering and medicine. Statistica provides a wide range of tools for analyzing data and creating high-quality graphs, as well as powerful data manipulation and statistical analysis capabilities.

7.1. Features of Statistica:

Data Analysis: Statistica provides a wide range of data analysis tools, including basic statistics, regression analysis, spectral analysis, design of experiments analysis, time series analysis, and multivariate data analysis.

Graphical visualization: Statistica can create a wide range of 2D and 3D graphs, including pie, line, and bar, surface, polar and 3D graphs.

Data processing: Statistica provides tools for data processing, including data transformation, data cleaning, data merging and data reshaping.

Statistical analysis: Statistica provides a wide range of statistical hypothesis tests, including t-test, analysis of variance, and chi-square tests.

Programming: Statistica supports a built-in programming language called Visual Basic for Applications (VBA), which allows users to create custom analysis and visualization tools.

7.2. User interface explained:

Statistic's user interface consists of the following windows:

- Project window This window is used to view currently open projects.
- Data window This window is used to view and analyze data.
- Graph window Use this window to create and edit graphs.
- Dashboard window Used to view and visualize data analysis options.
- Command Line Window This window is used to enter VBA commands.

7.3. How to use Statistica:

For basic use of Statistica, follow these steps:

- Import data Import your data from a file or enter it manually.

Analyze the data: Select the type of analysis you want to perform and apply it to your data.

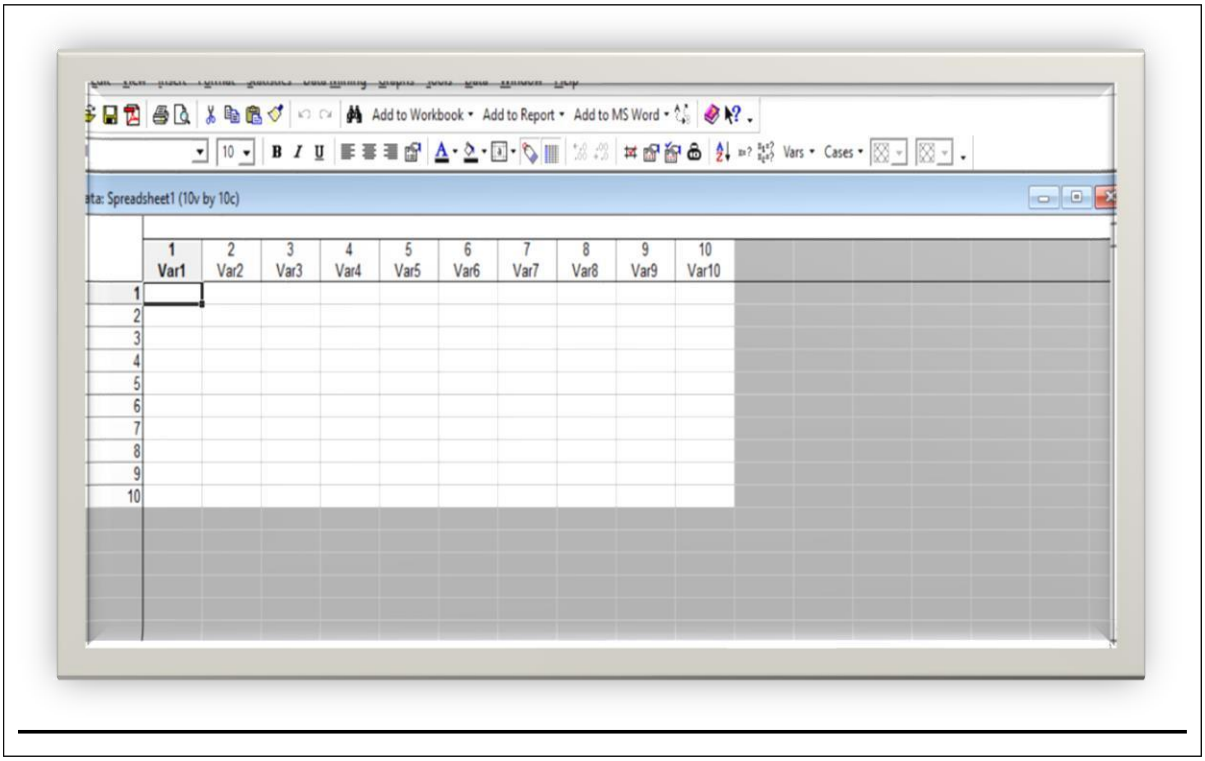

Fig.II.3. Statistica Application

8. Sequential Gaussian Simulation:

The sequential Gaussian simulation method is a means of interpolation (necessary for continuous data) by the data, which generates a distribution model based on variograms and trends (corresponding to the orientation observed for a series of data over a certain period).

This algorithm assumes that the data respects the following properties:

- Normal distribution, mean of values.
- Stationarity (the mean does not change laterally).
- No trend.

9. Object-based method

This method is suitable for channel simulation, as it models discrete data that is produced and distributed stochastically. All the values are entered: geometric form (length, width, thickness, curvature, etc.), the algorithm allows you to :

- Design the architecture and geometry of facies in a real way.
- Create objects based on predetermined shapes.
- Integrate channels and isolated objects.
- Analise vertical and lateral trends.

10. Petrophysical parameters and interpretations:

10.1Neutron logging (INPH):

High-speed neutrons (10,000 km/s) with energies of between 4 and 6 MeV are emitted by a radioactive source, generally Americium (Am)-Beryllium (Be), to bombard the formations traversed by the borehole. With each collision, these neutrons lose their energy, first reaching the epithermal stage (0.1 - 100 eV) and then the thermal neutron stage (around 0.025 eV).

10.2. Gamma Ray (GR) logging:

This is a record of the natural gamma radioactivity of the formations. The only radioactive elements with a significant concentration in natural materials are potassium, uranium and thorium. For sedimentary formations, significant radioactivity is recorded in:

- Clay formations containing potassium (especially illite).
- Potassium salts.
- Formations rich in organic matter can concentrate uranium.

- Detrital formations containing feldspar (potassium) or enriched in heavy minerals.

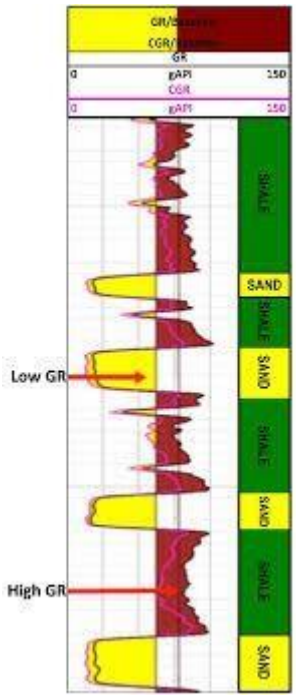

Fig.II.4. Gamma Ray (GR) logging

Applications:

1. Assess the porosity of reservoir rocks.

2. Identify lithology in combination with other tools.

3. Evaluate hydrocarbon density.

4. Good well-to-well correlation criteria

11. Permeability (K):

The permeability of a rock characterizes its ability to allow the flow of fluids contained in its pore space. The pore space only allows fluids to move insofar as the pores are connected to. each other, in which case it is said to be permeable.

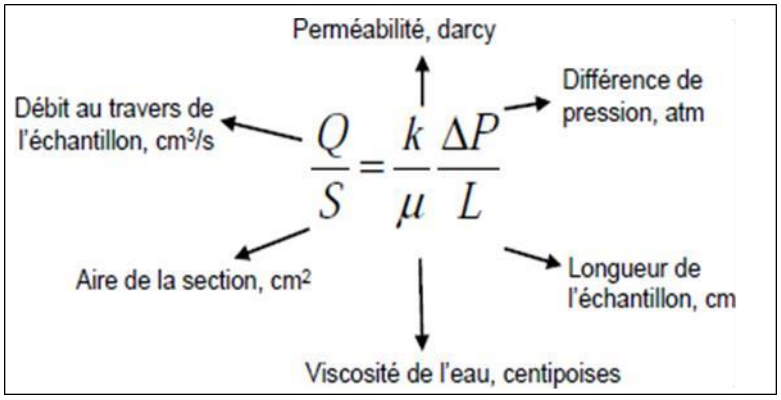

Fig.II.5. Darcy's law formula.

FIG.II.6. Ultra Perméamétre (In Sonatrach, 2010)[7].

12. Porosity (phit) (Φ):

corresponds to the total volume occupied by the voids in the rock (Vp) divided by the total volume of the rock (Vt); it is usually expressed as a percentage, but can also be found in the form of the fraction.

Fig.II.7. Measurement of solid volume (In Sonatrach, 2005)[8].

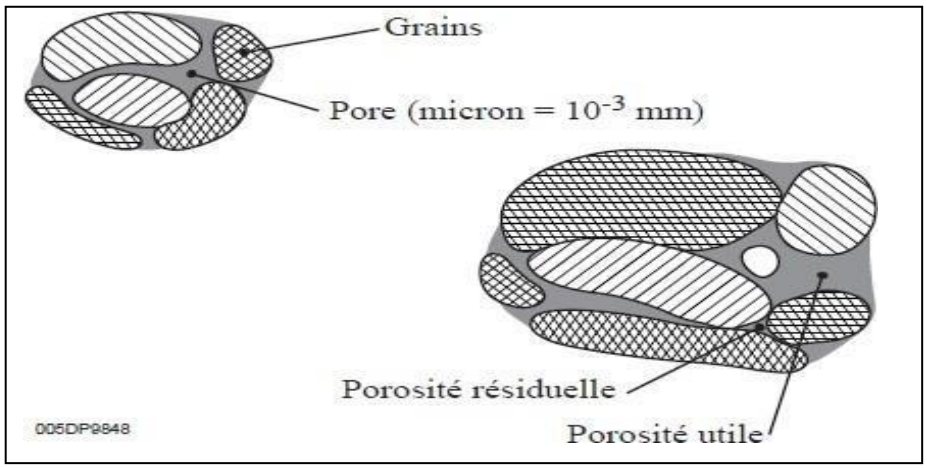

Fig.II.8. Porous medium (ENSPM, 2006)[9, 10]

13. Saturation:

In geology, "saturation" commonly refers to the degree to which a porous medium (such as soil or rock) is filled with water or other fluids. It is a crucial concept in understanding groundwater flow, petroleum reservoirs, and soil mechanics.

- ***Apparatus and Measurement Method:***

The Dean-Stark apparatus is a glass laboratory apparatus used in synthetic chemistry to extract water (or other liquids) from the reaction medium. It was invented by E. W. Dean and D. D. Stark in 1920. The apparatus, as depicted in Figure 15, comprises the following components:

- Sample holder
- Graduated test tube for the collection of water
- Vial of toluene
- Capacitor
- Battery (resistant to toluene boiling)

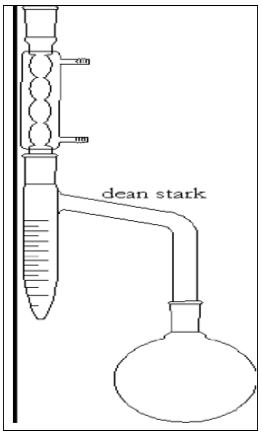

Fig.II.9. Diagram presenting the DEAN STARK method (Chemo, 2003)[11].

- **Water Saturation:**

  This refers to the proportion of pore space within a rock or soil that is filled with water. It is a critical parameter in hydrogeology, as it affects the movement of groundwater and the storage capacity of aquifers.

- **Saturation in Petroleum Geology:**

In the context of petroleum exploration and production, saturation typically refers to fluid saturation within reservoir rocks. Petroleum reservoirs contain a mixture of oil, gas, and water, and understanding the saturation levels of each fluid phase is essential for estimating reserves and optimizing production.

- **Saturation in Soil Mechanics:**

In soil mechanics, saturation refers to the state where the voids or pores in a soil are filled with water, leaving no air. Saturation affects soil strength, permeability, and compressibility, and is a crucial factor in geotechnical engineering for evaluating slope stability, foundation design, and groundwater flow.

- **Saturation Excess Overland Flow:**

This concept is related to surface water hydrology, where saturation excess overland flow occurs when rainfall exceeds the infiltration capacity of the soil, leading to surface runoff. This process is important for understanding flood generation and runoff mechanisms in watersheds.

In each of these contexts, saturation plays a vital role in determining the behavior of fluids within geological materials and has implications for various geological processes and engineering applications.

14. Classification of petrophysical parameters:

Petrophysical parameters are the physical properties of rocks that are used to characterize oil and gas reservoirs. They are generally classified according to their nature and their use in the oil industry. Here is a common classification of petrophysical parameters[10]:

14.1. Porosity parameters:

- **Total porosity:** The fraction of the volume of a rock that is composed of empty spaces (pores).
- **Effective porosity:** The portion of total porosity that contains mobile fluids and can contribute to the production of hydrocarbons.
- **Unconnected porosity:** Pores that are isolated and not in communication with other pores, often filled with immobilized water.

14.2. Permeability parameters:

- **Absolute permeability:** The ability of a rock to allow the flow of fluids through its pores.
- **Relative permeability:** The permeability of one fluid relative to another fluid, often expressed as a function of fluid saturation in the rock.

14.3. Saturation parameters:

- **Water saturation:** The fraction of the pore volume filled with water.
- **Oil saturation:** The fraction of the pore volume filled with oil.
- **Gas saturation:** The fraction of the pore volume filled with gas.

14.4. Electrical Conductivity Parameters:

- **Resistivity:** The ability of a rock to resist the passage of an electric current, often used to characterize the fluids present in the rock.

14.5. Density parameters:

- **Rock density:** The mass per unit volume of the rock.
- **Fluid density:** The mass per unit volume of fluids presents in the rock, such as water, oil and gas.

14.6. Composition parameters:

- **Mineralogy:** The mineralogical composition of the rock, which can influence its physical properties.
- **Texture:** The size, shape and distribution of the rock's constituent grains, which affect its permeability and porosity.

These parameters are essential for assessing the quality and productivity of an oil or gas reservoir, and for guiding exploration, drilling and production decisions in the oil industry.

15. Methods of measurement and analysis:

These are physical characteristics of rocks or porous materials found underground, often used in the oil and gas industry to evaluate oil and gas reservoirs. The following is a general approach to the method of measuring these parameters:

15.1. Analysis of rock samples (cores):

Drill core samples are taken from wells and analyzed in the laboratory to determine various petrophysical parameters such as porosity, permeability, fluid saturation, etc.

15.2. In-situ measurements:

- **Electrical logging:** Logging tools such as neutron probes, density probes and electrical probes are used to measure porosity, fluid saturation and other parameters.
- **Nuclear logging:** Measurement of porosity and density of fluids using radioactive sources and detectors.
- **Acoustic logging:** Measurements of the speed of sound waves in the formation to estimate lithology and porosity.

15.3. Laboratory tests:

Specific tests can be carried out on rock samples to obtain more detailed data, such as permeability tests, resistivity tests, porosity tests, etc.

15.4. Data modelling and interpretation:

Once the data has been collected, it is analyzed and interpreted to characterize the reservoir and estimate important petrophysical properties such as fluid storage capacity, permeability, etc.

15.5. Field validation:

The data obtained is often validated by actual field production tests to confirm the accuracy of the petrophysical estimates and improve the reservoir models.

This approach combines direct and indirect measurement methods to obtain a complete picture of the petrophysical properties of a reservoir, which is essential for making informed decisions about oil and gas exploration and production

16. Measurement of parameter petrophysical:

16.1. Measurement of porosity:

Porosity is the set of voids (pores) in a material that are filled by fluids (liquids or gases). Porous materials are very generally solids, but there are also porous liquids and assemblies that are porous, such as piles of grains or powders. Porosity is also a physical quantity defined as the ratio between the volume of voids and the total volume of a porous medium. Its value is between 0 and 1 (or, in percentage terms, between 0 and 100%)[10]:

$$\varphi = \frac{V_{pores}}{V_{Total}} \qquad \text{Eq.1}$$

$\boldsymbol{\varphi}$ is the porosity.

$\boldsymbol{V}$ pores the volume of pores.

$\boldsymbol{V}$ total the total volume of the material, i.e. the sum of the solid volume and the pore volume.

The porosity of a substrate determines its flow and retention capacities (see also Darcy's Law).

16.2. Measurement of permeability:

- Permeability is defined as the ability of a rock to allow a fluid to pass through its pore space.
- The analysis is carried out on samples measuring 1″ or 1.5″ in diameter by 1.5″ in length.

- The permeability measurement under laboratory conditions is carried out at a confining pressure of 200 psi or 400 psi.

Permeability (using a conventional permeameter) is measured and calculated using an equation derived from Darcy's law[12, 13]:

$$K_a = \frac{CQHL}{200 \cdot S} \qquad \text{Eq.2}$$

S: Cross-sectional area

L: Length

Q: Flow rate

H: Height

***C*: Constant**

16.3.Measurement of Saturation:

In the context of rocks, saturation typically refers to the degree to which the pore spaces within the rock are filled with fluids, usually water or hydrocarbons. Saturation is an important property in fields such as petroleum geology, hydrogeology, and reservoir engineering, as it affects the flow of fluids through the rock.

There are several methods used to measure the saturation of rocks:

16.3.1 Laboratory Core Analysis: In this method, rock core samples are extracted from the subsurface and brought to the laboratory for analysis. Various techniques can be employed to measure the saturation of the core samples, including:

- **Core Saturation Measurements:** The core samples are saturated with a known fluid (e.g., water or oil), and then the fluid content is measured using techniques such as gravimetric analysis or nuclear magnetic resonance (NMR).
- **Capillary Pressure Measurements:** Capillary pressure measurements are used to determine the relationship between the saturation of different fluids (e.g., water and oil) within the rock pores. This information can be used to calculate the saturation of each fluid phase in the reservoir.

16.3.2. Well logging: Well logging tools are used to measure various properties of the rocks in situ, including their saturation. Gamma ray, neutron, and density logs are commonly used to estimate porosity and saturation in boreholes[14].

16.3.3. Petrophysical Models: Petrophysical models use measurements of rock properties such as porosity, permeability, and mineralogy to estimate saturation indirectly. These models often rely on empirical relationships derived from laboratory core analysis data.

16.3.4. Geophysical Imaging: Geophysical methods such as seismic imaging and electromagnetic surveys can provide indirect measurements of rock saturation by detecting changes in the physical properties of the subsurface associated with fluid presence.

Each method has its advantages and limitations, and the choice of method depends on factors such as the type of rock, the availability of core samples, and the desired level of accuracy. In practical applications, a combination of methods is often used to obtain a more comprehensive understanding of rock saturation in subsurface reservoirs.

17. Measuring saturation: There are three laws for measuring saturation

Measuring the saturation of water[15]:

Water saturation, expressed as a percentage, is then calculated using the following formula:

$$S_w(\%) = \frac{V_b}{V_p} \times 100 \qquad \text{Eq.3}$$

Oil saturation expressed as a percentage is calculated using the following formula:

$$S_o(\%) = \frac{X_b}{V_p} \times 100 \qquad \text{Eq.4}$$

Chapter III: Results analysis and interpretation

1. Introduction to the field of study:

The evolution of well pressures as a function of production has made it possible to subdivide the Hassi Messaoud deposit into 25 so-called production zones of variable extension.

These zones are relatively independent and correspond to a group of wells that are in communication with each other and not with neighboring zones.

They each have their own behavior in terms of reservoir pressure ().

Our study will focus on Area 23, which is located in the south-west of the Hassi Messaoud field, as shown in the following figure:

Area 23 is located in the south-west of the Hassi Messaoud oil field, bounded to the north by Area 2ex, to the west by Area 1b and to the south by no oil field, although this area is smaller in size than the others.

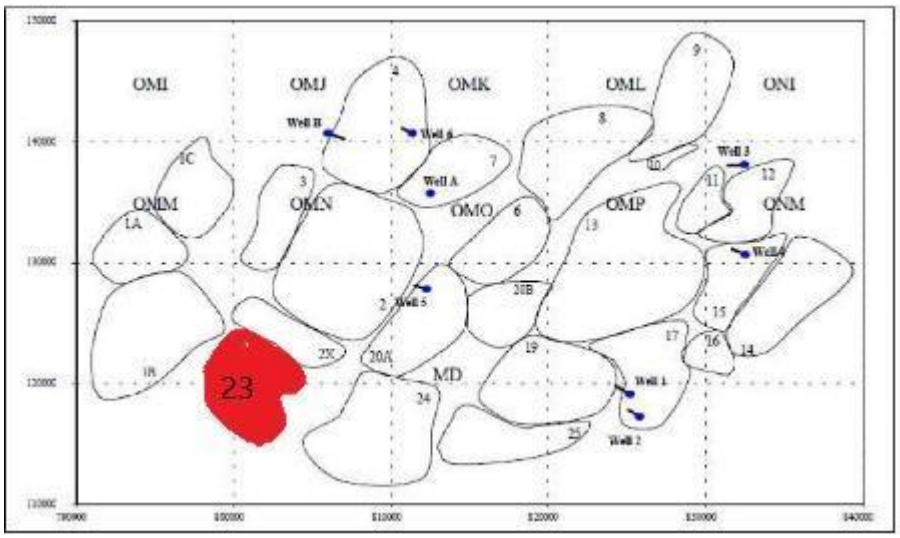

Fig.III.1. Zoning map of the Hassi Messaoud field[5, 16].

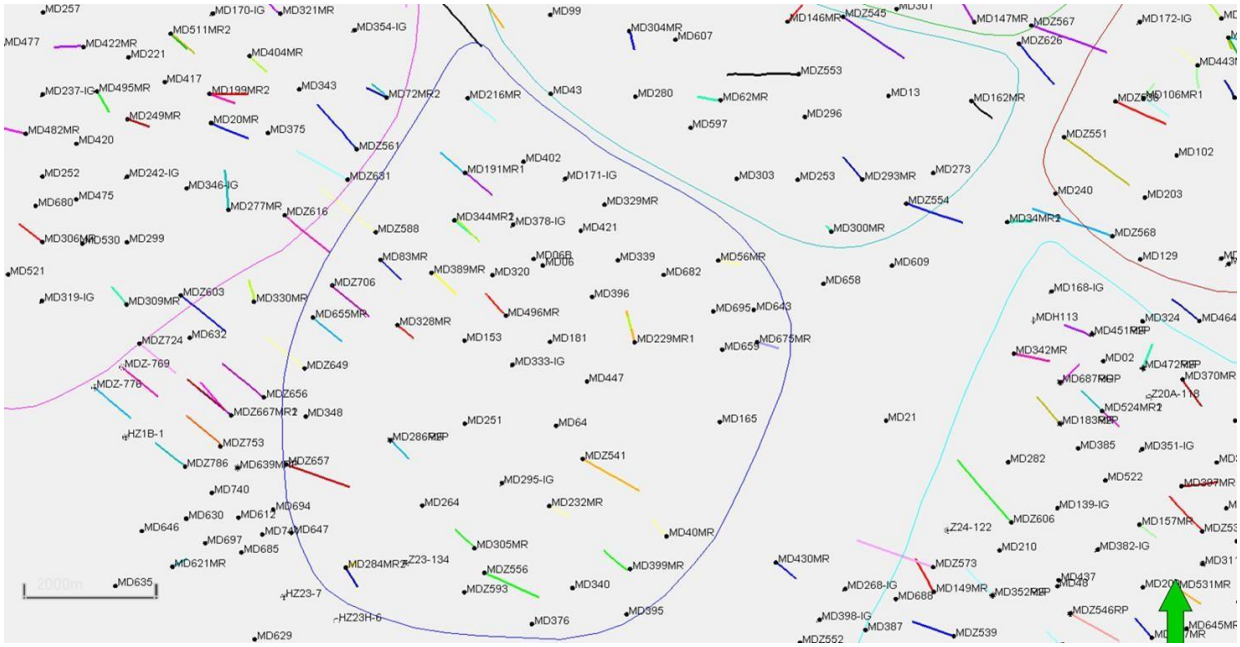

Fig.III.2. Position of wells in zone 23[2].

2. Structural and petrophysical studies for the southwest sector of Area 23 (Hassi Messaoud):

The southwest sector of Area 23 is structurally shown as a monocline and is located on the southwest periphery of the Hassi Messaoud field where the effects of unconformity due to erosion are very strong and the banks are successively eroded to the unconformity surface. The main results obtained from this study are summarized below:

Structural and petrophysical modelling was carried out using the Schlumberger Petrel tool and shows the following points:

- The structural model of the S-W sector of Area 23 is intersected by several faults, including a major northeast-west trending fault with a 30 m rejection.
- Hercynian erosion has affected the Ordovician (red quartzite)
- Geological cross-sections and correlations in different directions enabled us to highlight the monolithic structure of the reservoir in the study area and follow the variation in the thickness of the different drains. The structural model was then populated with petrophysical properties leading to the following results:

Creating a three-dimensional model of the petrophysical parameters in all banks of the reservoir of the sector gave us information on the spatial evolution of these parameters.

After analyzing the reservoir property maps, we can conclude that the petrophysical parameters, i.e. porosity and permeability, are generally medium and sometimes low. In general, porosity varies according to a natural law, indicating the homogeneous nature of its distribution.

Porosity in the Cambrian reservoir is medium, ranging from 5% to 8%. Permeability is low to moderate in the reservoir and very low in D3. The permeability of the matrix ranges from 0.1 m/d to 1 m/d. According to the petrophysical study, the best characteristics of the reservoir are found in the southeast and northeast sectors. The best drainage areas correspond to the RI-inf, D4 and to a lesser extent D3 drains which have poor to poor properties. The theoretical water level is approximately between 3360 m and 3380 m.

3. Cylindrical tracks and interpretation:

MD284 sediment-stratigraphy description:

(3350m-3356m) md284:

Fig.III.3. carrot of md 284

Grey-green to light grey quartzites with very fine siliceous or silico-argillaceous cement; admits numerous ‘cm’ to ‘mm’ green clay passages.

Locally dark grey, numerous flat Tigillites, especially at clay joints.

Sub horizontal cracking open to closed wedge empty or clogged with clay.

Sub horizontal stratification Surtement media ere

(3382m-3387m) md284: Alternation

Fig.III.4. carrot of md 284 alternation.

Light grey to dark grey clay; soft to slightly unconsolidated clay and sandstone. Grey-green soft to very soft. Soft. Moderately hard clay or siliceous clay cement.

Numerous CCD sandstone nodules in clay layers.

(3397m-3399m):

Fig.III.5. carrot of md 284 silty

Black clay. Silty ± indurated admitting very few ‘mm’ to ‘cm’ passes of very fine light grey, probably glauconitic.

(3405,50m-3408m):

Fig.III.6. carrot of md Silty clay, grey-black locally grey-green.

Silty clay, grey-black locally grey-green.

Rare ‘mm’ ET. Da layers of very fine light grey to greenish grey sandstone, probably glauconitic.

(3469m-3472m):

Fig.III.7. carrot of md284. Dark grey isometric quartzite-grey

Dark grey isometric quartzite-grey with numerous Tigillites showing festooned figures.

Rare stylistic joints.

(3519m-3522m):

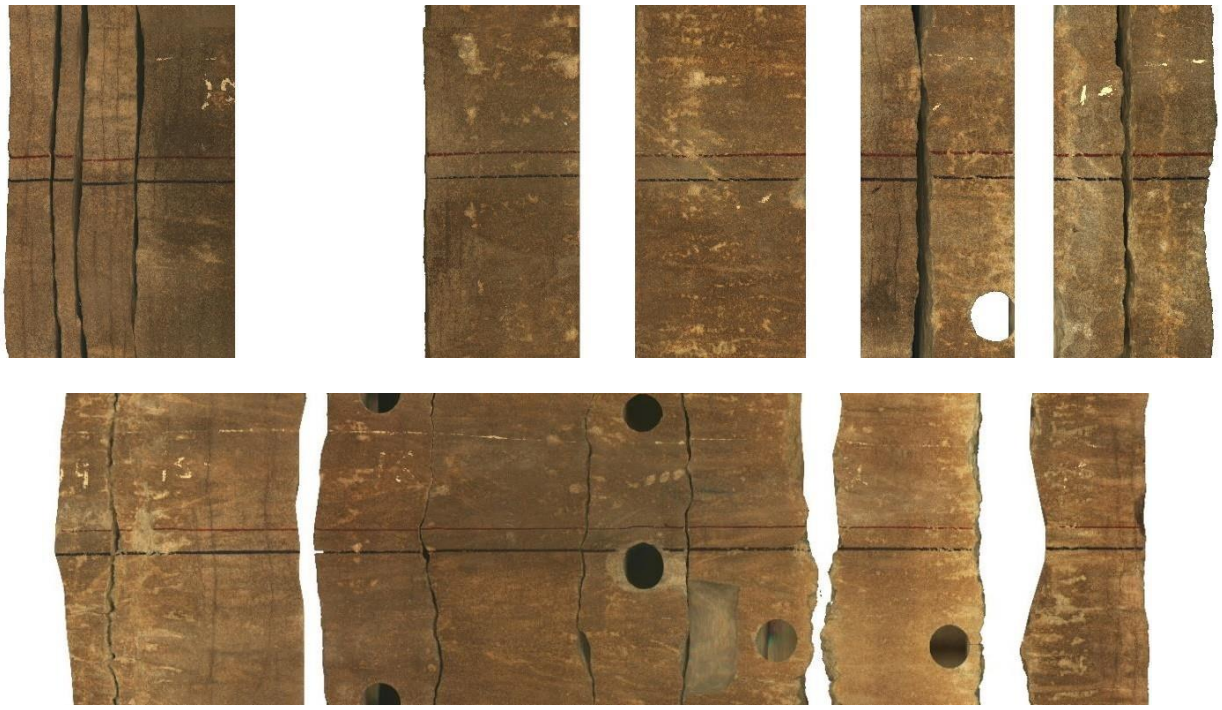

Fig.III.8. carrot of md284. Anisometric siliceous grey-beige quartzite.

Medium to coarse anisometric siliceous grey-beige quartzite sandstone becoming yellowish silico-clay admitting a centimetric layer and a few lithic stylistic joints of greenish grey clay.

Cracking: horizontal developed Indications none

4. ***The isopermiability, isoporosity and saturation maps for D1, D2, D3, D4 and D5 ID are presented below:***

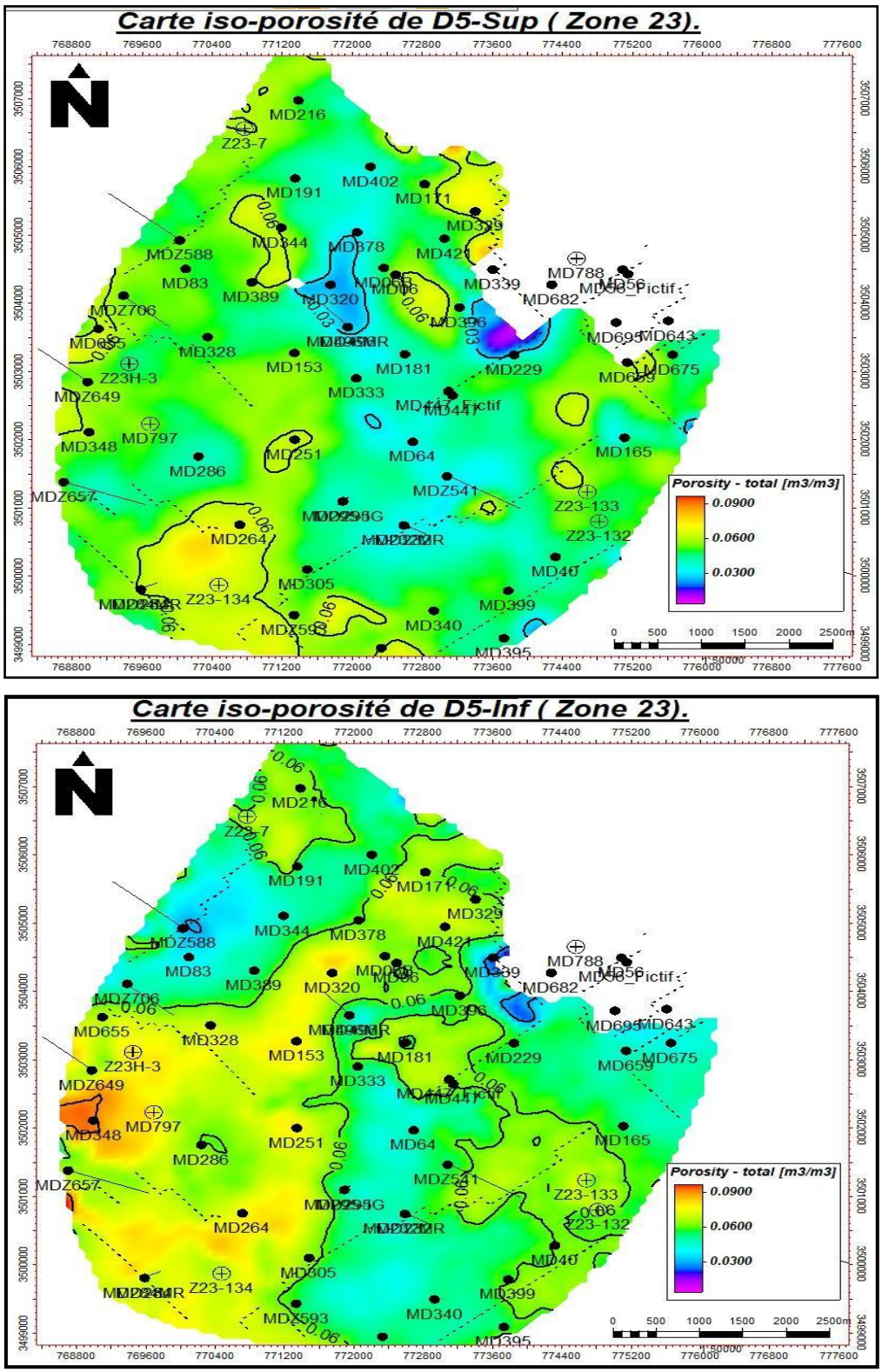

Fig.III.9. structural map iso porosity Internal and external of the D5

Commentary and explanation of the iso-porosity map (D5 sup):

It is observed that the lowest porosity values are concentrated in the region between the wells (MD229, MD682, MD339, and MD396), precisely to the north of well MD229. Conversely, the highest values are found between the wells (MD269 and Z23-134) on the west side of the two wells. Finally, it is observed that the mean porosity distribution is in close proximity to the mean values across the entire study area.

Commentary and explanation of the iso-porosity map (D5inf):

We note that porosity is high at MD348, MDZ629 up to 0.09% in the south-east, low at MD682 and MD339 in the south-west and moderate or close to 0.03-0.05% in the rest of the region such as MD340, MD64 and MD333.

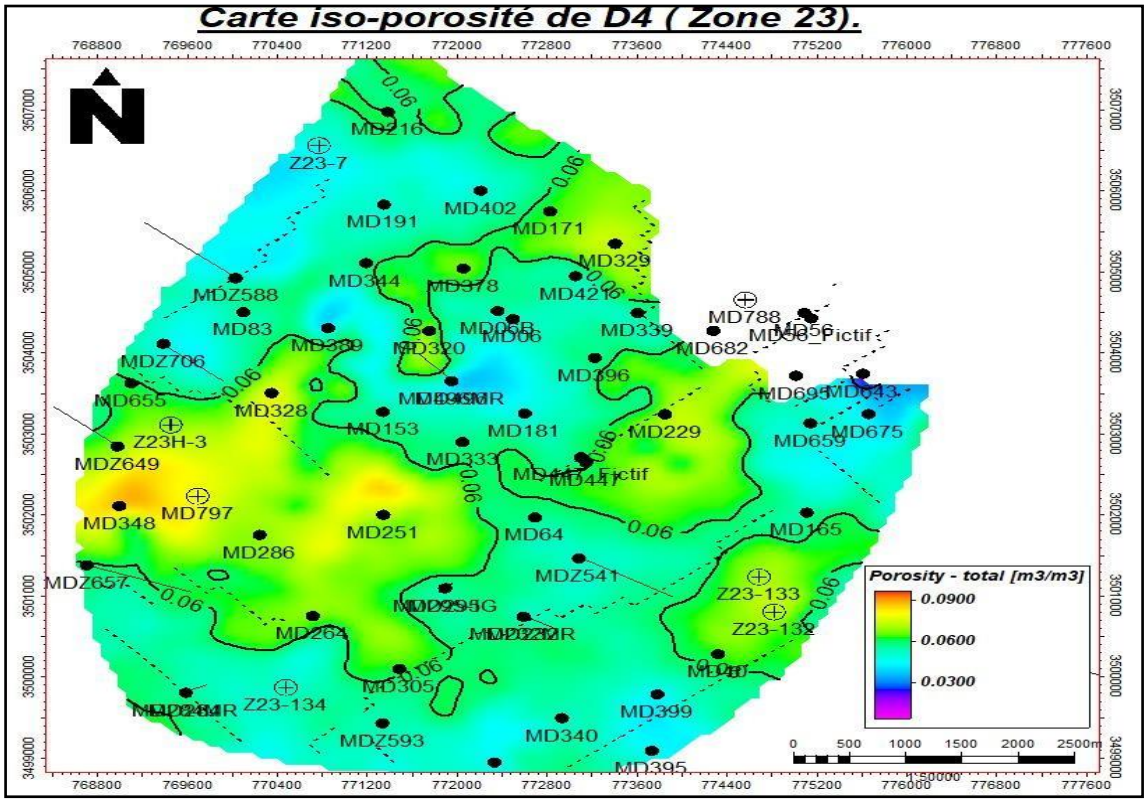

Fig.III.10. structural map iso-porosity of the D4(Area23).

Commentary and explanation of the iso-porosity map D4:

The map shows the distribution of porosity in Area 23 at D4, where porosity is high in the southwest, specifically at MD348 MDZ649, reaching 0.09%, while it is low in the southeast at MD643 MD675, reaching 0.03%, and close in the rest of the area between 0.04 and 0.06%.

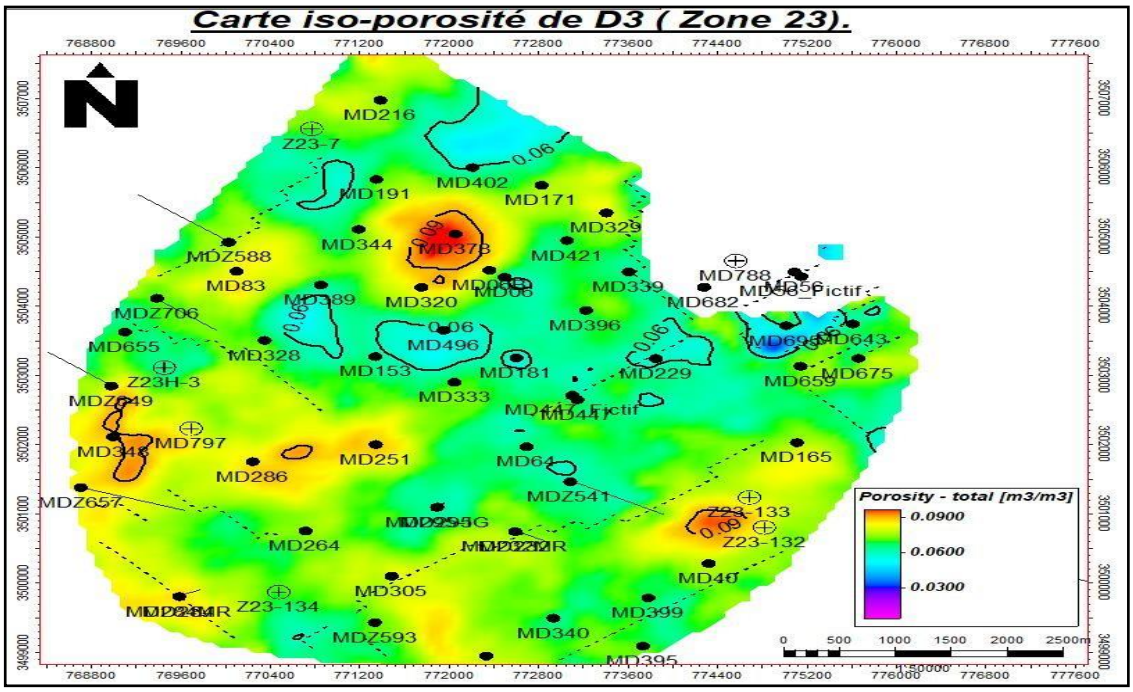

Fig.III.11. structural map iso-porosity of the D3 (Area23)

Commentary and explanation of the iso-porosity map D3:

It is noted that the lowest porosity values are concentrated in MD 695 and, on the contrary, the highest values between the two holes (MD378 and Z23-132) are located on the eastern side of the two holes. Finally, it is noted that the average porosity distribution is close to the average values for the entire survey area.

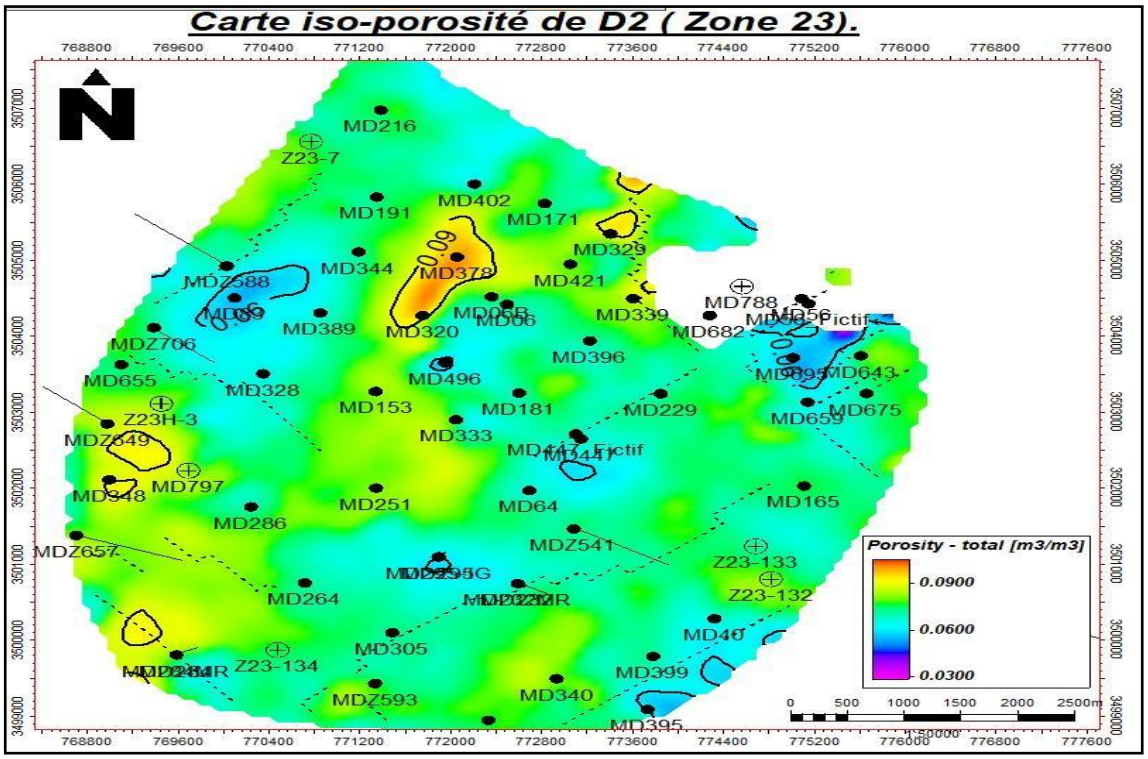

Fig.III.12. structural map iso-porosity of the D2 (Area23)

Commentary and explanation of the iso-porosity map D2:

The map shows the porosity distribution in D2.

MD378 is high in the north, while MD895 is very low at 0.03%, with the rest of the area close to 0.04-0.06%.

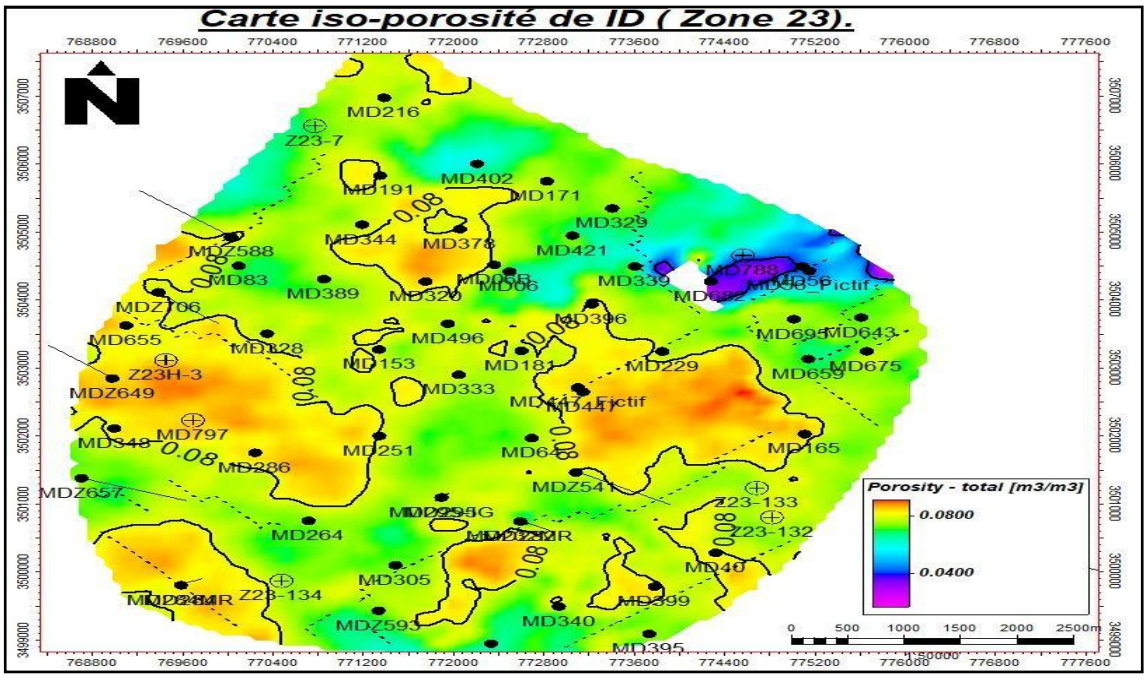

Fig.III.13. structural map iso-porosity of the ID(Area23).

Commentary and explanation of the iso-porosity map ID:

The map shows the distribution of porosity in the ID and we can see that it is high in most of the region, except in the northeast where we find low porosity at MD768.

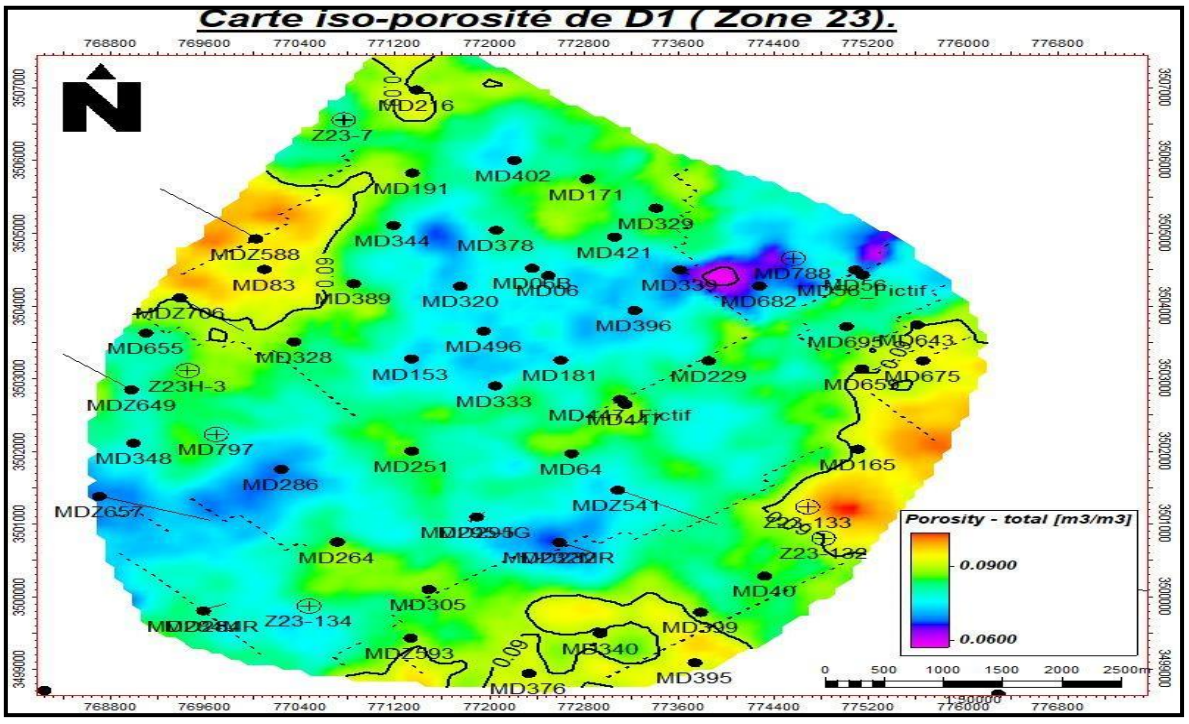

Fig.III.14. structural map iso-porosity of the D1(Area23).

Commentary and explanation of the iso-porosity map D1:

The map shows the distribution of porosity in D1, where we can see that porosity is low in the center of the region and high southeast of MD165 and northwest of MDZ588.

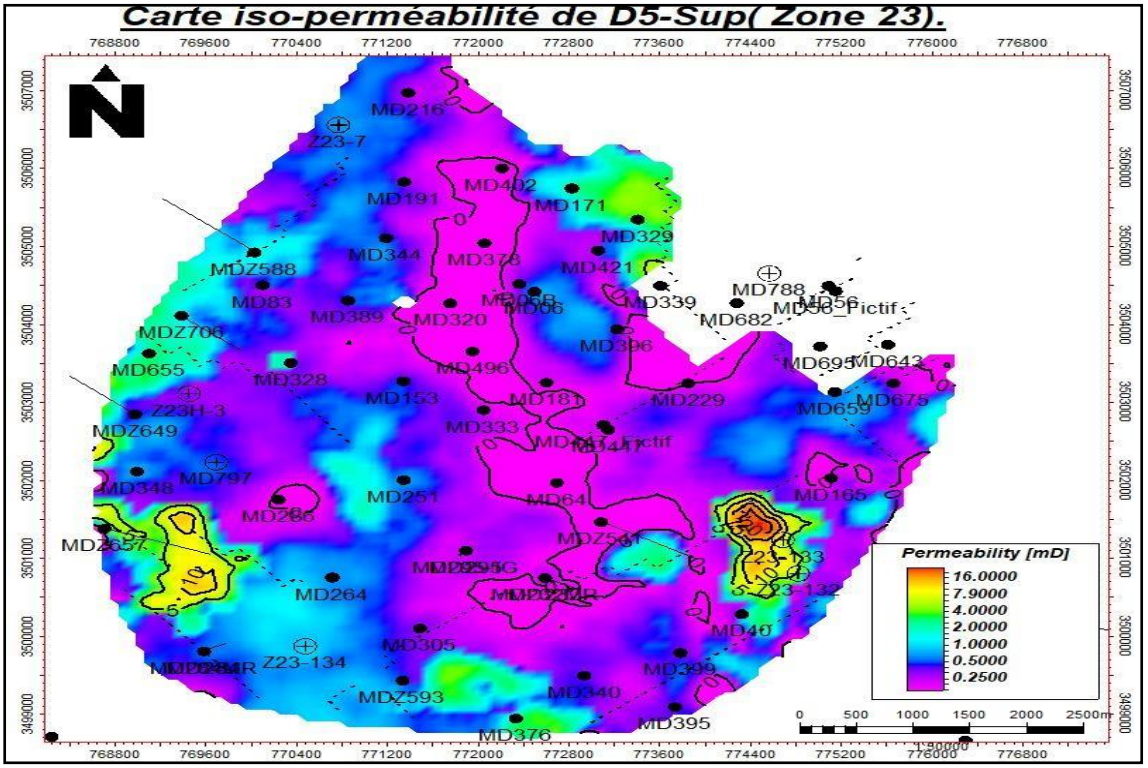

Fig.III.15. structural map iso-Perméabity of the D5 Super (Area23).

Commentary and explanation of the iso-Permeability of D5 Super

The map shows the distribution of permeability in the D5super, where we can see that permeability is low throughout the region and high in the southeast at Z23-133.

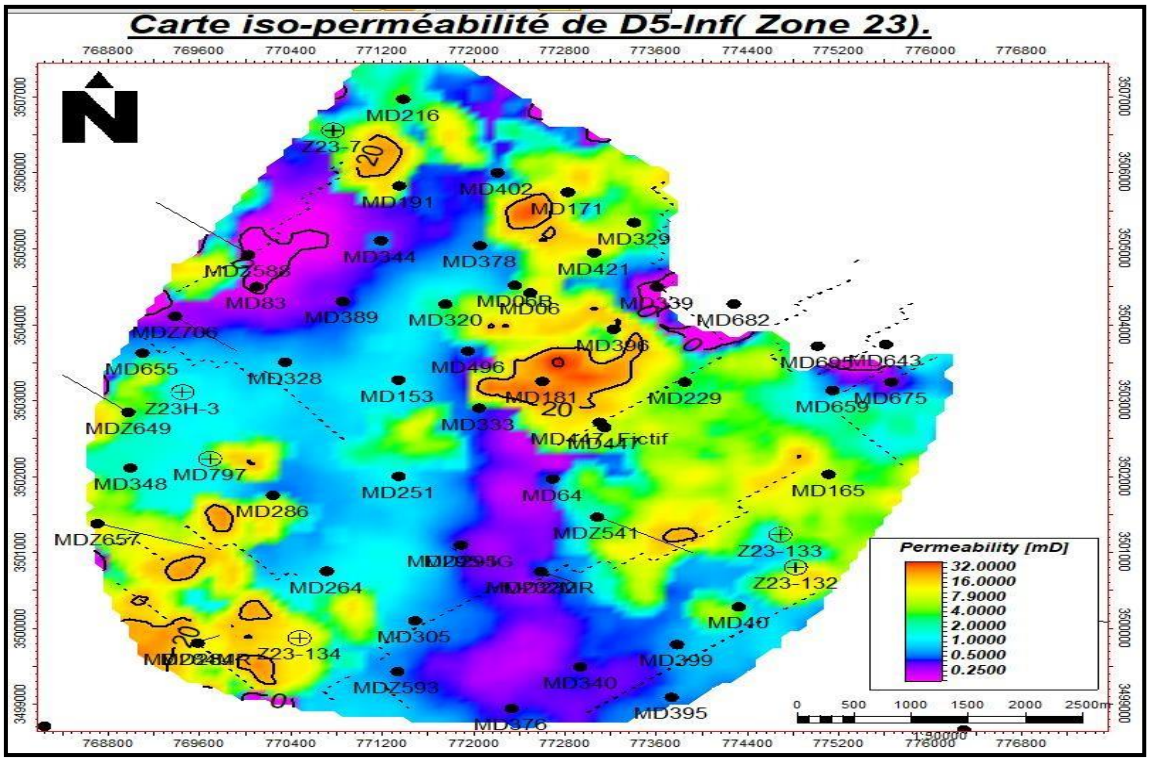

Fig.III.16. structural map iso-Perméabity of the D5 infer (Area23).

Commentary and explanation of the iso-Permeability of D5 infer:

The map illustrates the distribution of permeability in D5 Inf. It can be observed that the region exhibits a heterogeneous distribution of permeability, with high ratios observed at MD181 and MD171 in the north and Z23-134 in the southwest, and very low ratios observed in the northwest and south of MD64.

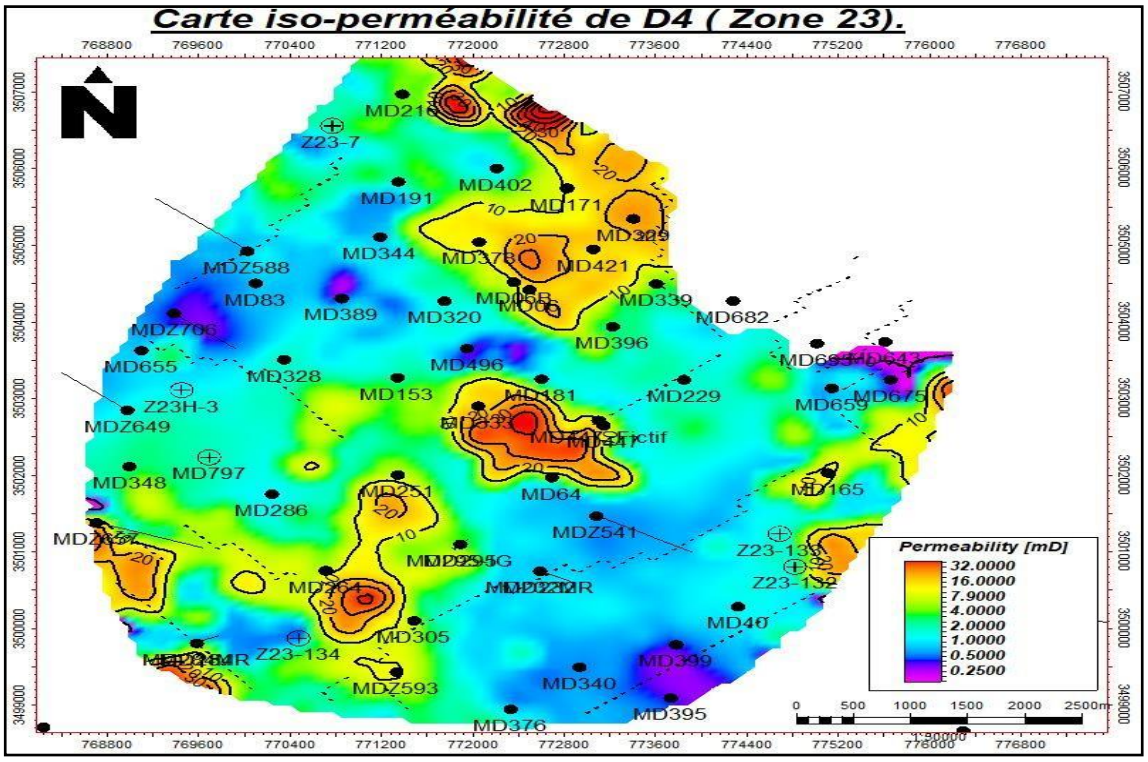

Fig.III.17. structural map iso-Peméabity of the D4 (Area23).

Commentary and explanation of the iso-Permeability of D4:

The map shows the distribution of permeability at the center of MD64, MD181 and MD264. MD421. MD216, very low at MD643.MD399 and converging in the rest of the region.

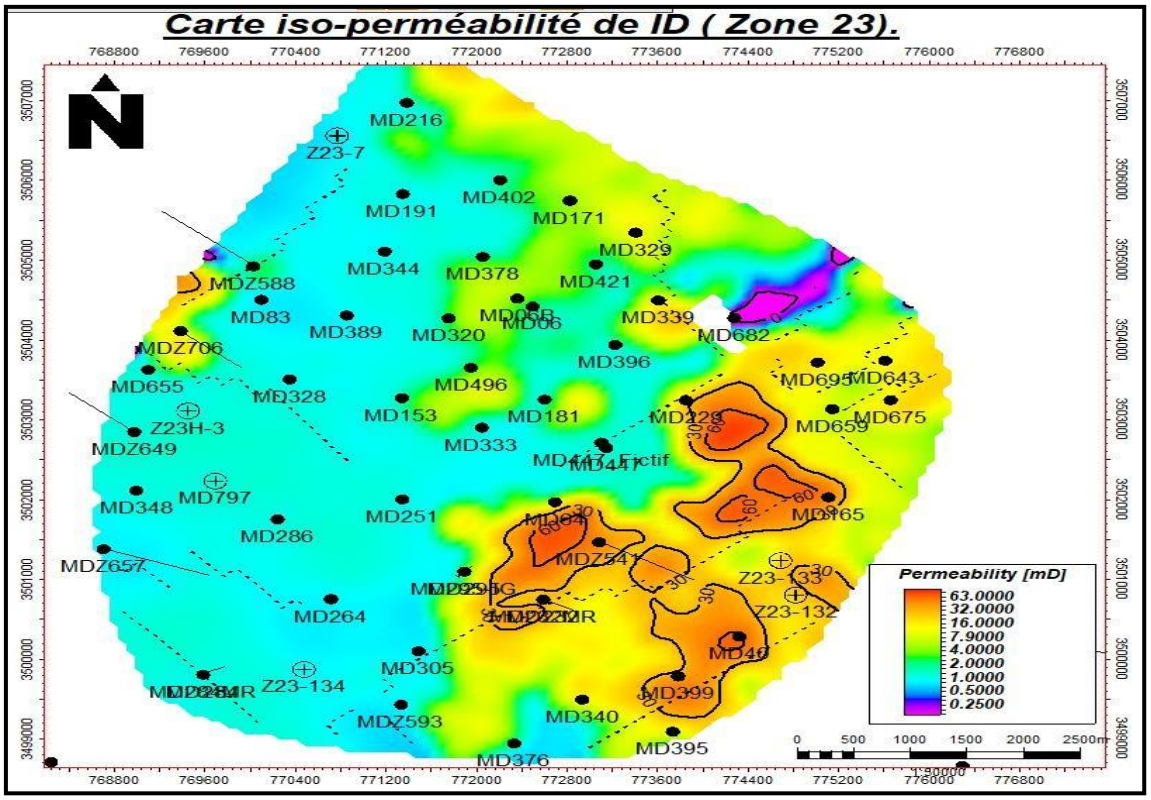

Fig.III.18. structural map iso-Perméabity of the ID(Area23).

Commentary and explanation of the iso-Permeability of ID

The map shows the distribution of permeability in ID, where we can see that it is high in the southeast, especially at MD229 .MD46 .MD229. It reaches 63% and decreases at MD682, which is quite low, and also in the west.

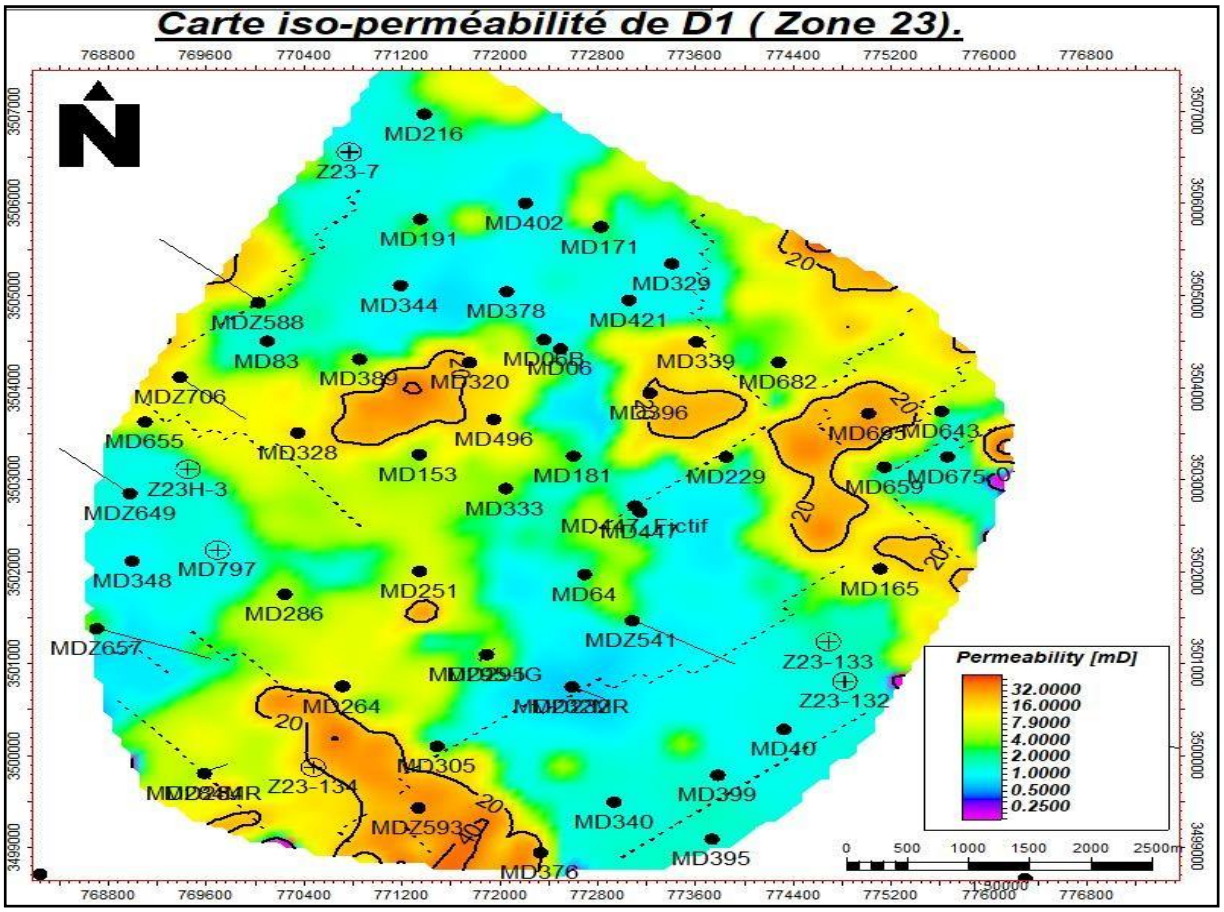

Fig.III.19. structural map iso-Perméabity of the D1 (Area23).

***Commentary and explanation of the iso-Permeability of D1*:**

The permeability map at D1

Permeability increases at MD593.MD320.MD396.

It is low at MD40.MD340 and low in the rest of the region, especially to the west.

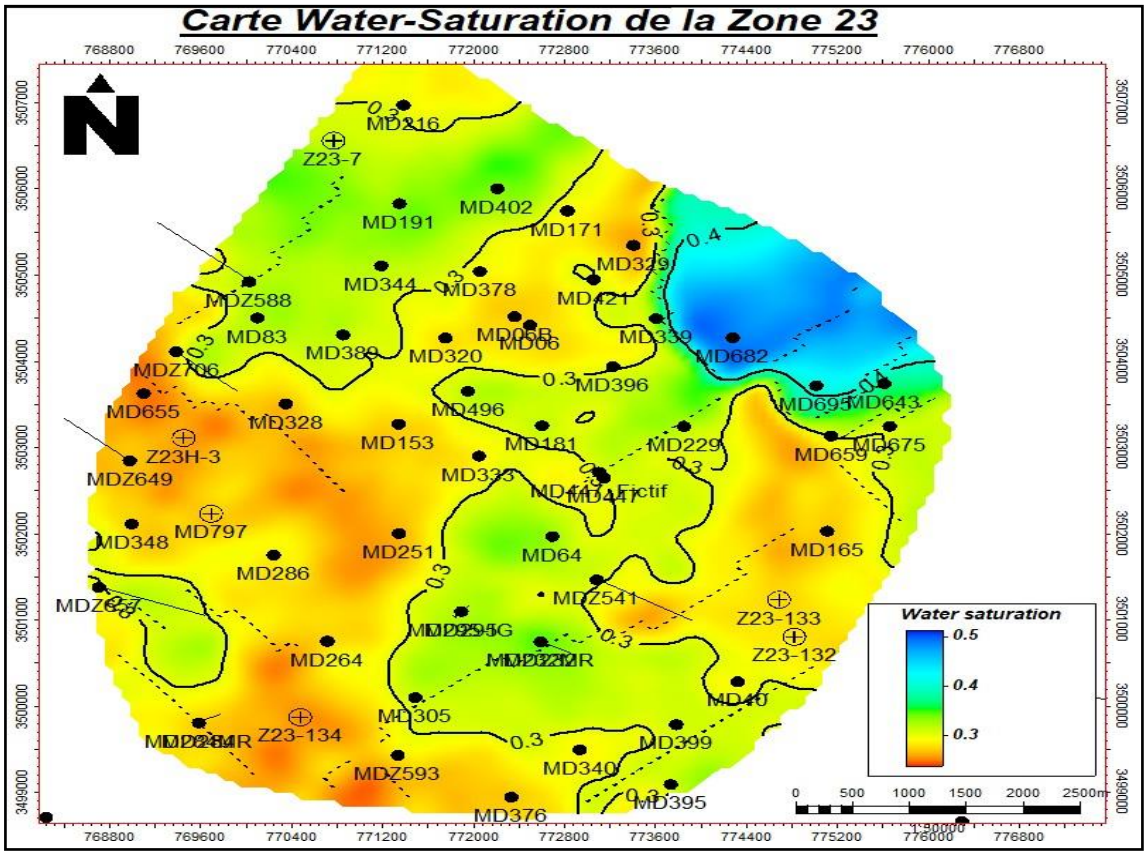

Fig.III.20. structural map Saturation the (Area23).

Commentary of map saturation the (Area23):

Map shows saturation of Area 23, noting lack of saturation similar to Far East on MD682.

5. Curves of porosity and permeability for wellsMD64.MD83.

MD171.MD181.MD191:

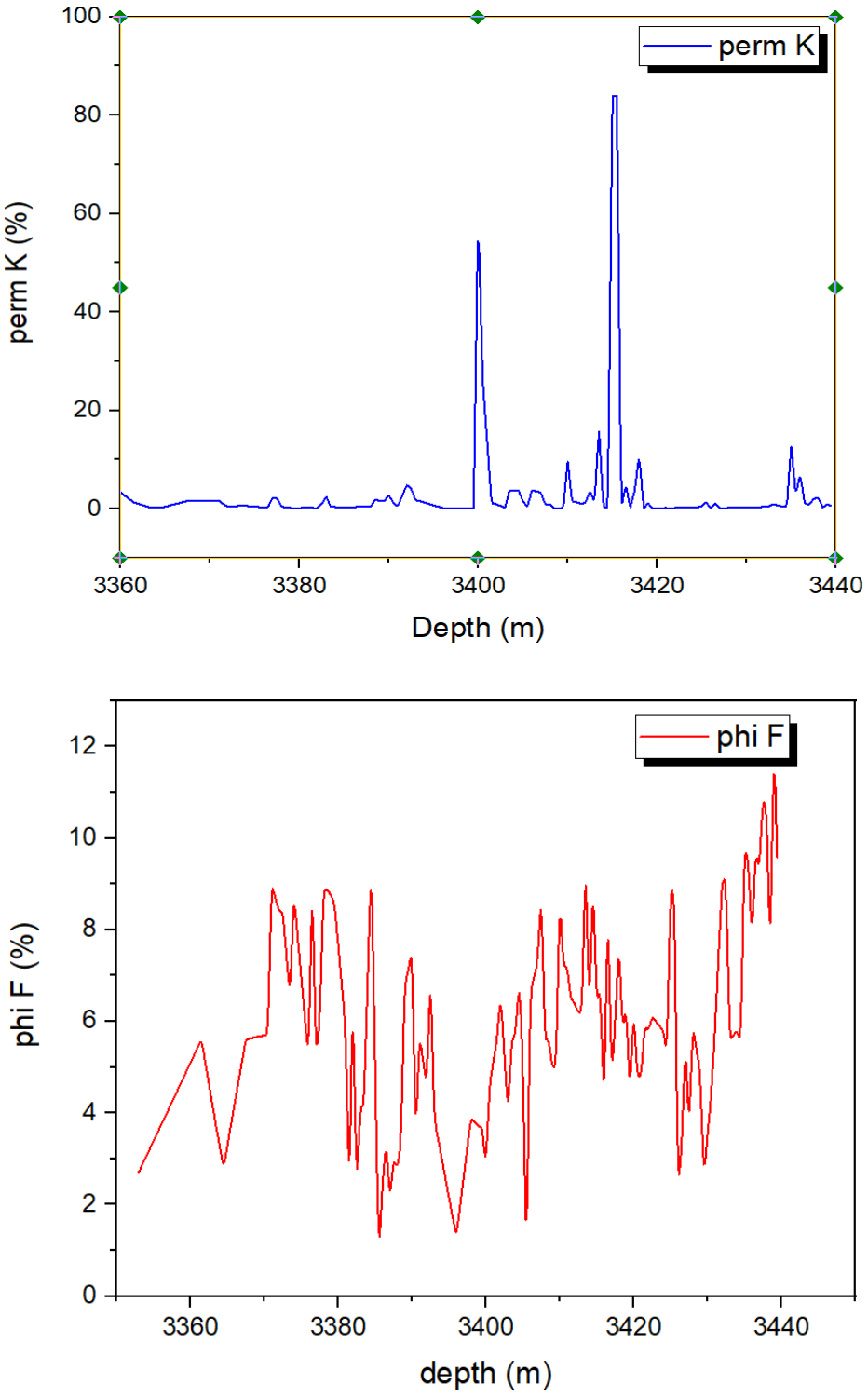

Fig.III.21. curve represents the values of the porosity and permeability changes in well MD64.

Commentary:

The image depicts two graphs representing the relationship between the depth of a material and its phi F value. The first graph illustrates the relationship between the depth of a material and its perm K value, while the second graph depicts the relationship between the depth of a material and the value of phi F.

Analysis:

This decrease could be attributed to an increase in the density of the material or a change in its composition as its depth increases.

Second graph:

The phi F value shows a sharp decrease as the depth of the material increases.

This decrease indicates a decrease in the alkalinity of the material as its depth increases.

The material depicted in these graphs could be soil, sediment, or another type of solid. The change in the value of perm "K" and Phi"Φ" with the depth of the material could be due to multiple factors, such as changes in pressure and composition. As the depth of the material increases, the pressure on the material increases. This pressure can lead to a change in the permeability and alkalinity of the material. Additionally, as the depth of a material increases, its chemical composition can change. This change can result in alterations to the permeability and alkalinity of the material.

The presence of other compounds can also influence the permeability and alkalinity of the material, as these compounds may react with water or with each other.

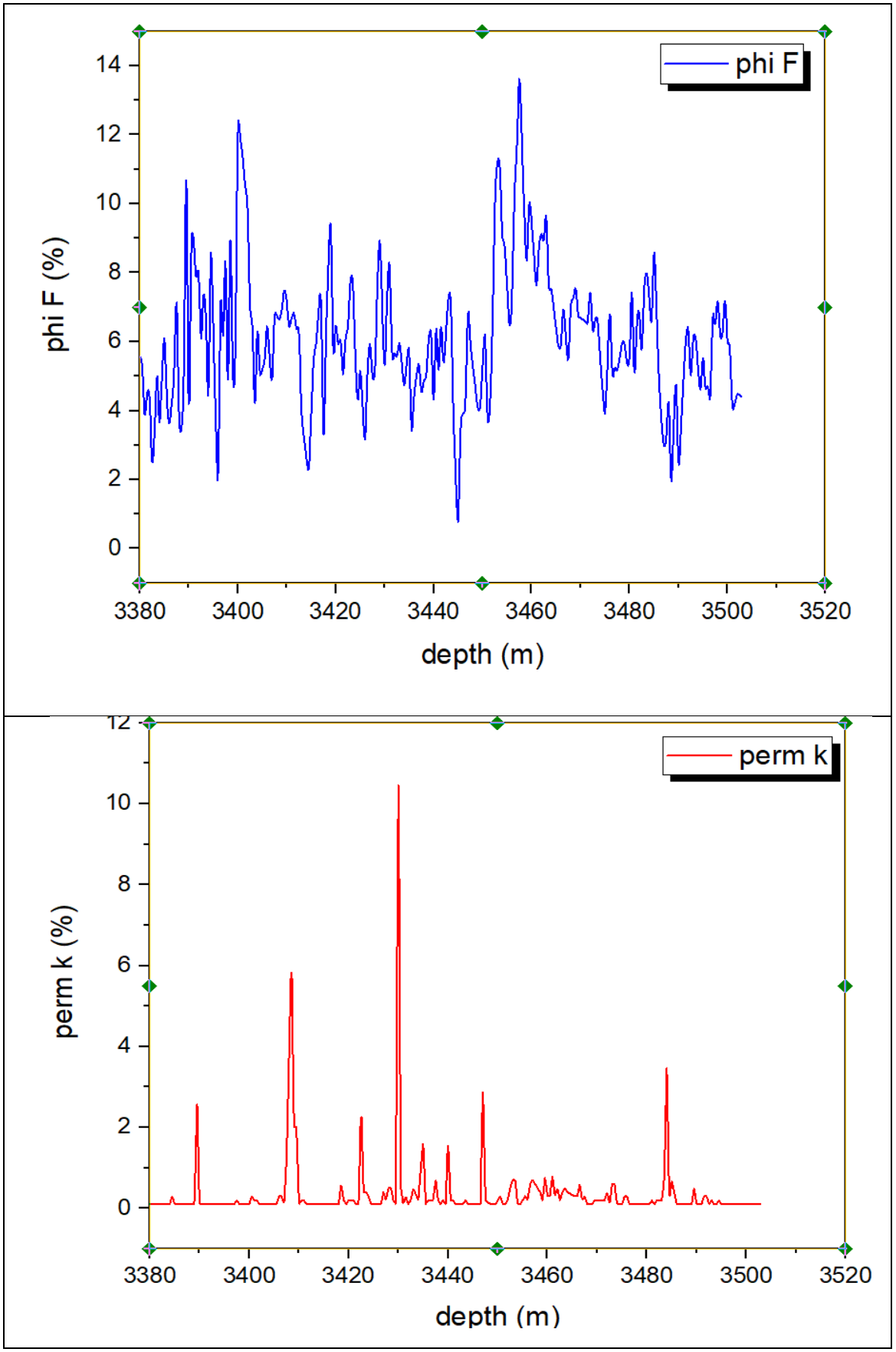

Fig.III.22. curve represents the values of the porosity and permeability changes in well MD83

Commentary:

The objective of this analysis is to examine the relationship between the variable phi"Φ" and the variable depth (m).

The relationship between the variable phi "Φ"and the variable depth (m) is as follows:

The matrix indicates an inverse relationship between the variables phi "Φ" and depth (m).

This indicates that as the depth of the material increases, the value of phi "Φ" decreases.

This relationship can be analyzed using a linear regression model.

The relationship between the variable perm "k" and the variable depth (m) is as follows:

The matrix indicates an inverse relationship between perm "k" and depth (m).

Consequently, as the depth of the material increases, the value of perm "k" decreases.

This relationship can be analyzed using a linear regression model.

Potential explanations for this phenomenon include:

The variable phi"Φ" is believed to represent the alkalinity of the material.

A reduction in the value of phi"Φ" as the depth of the material increases suggests that the alkalinity of the material diminishes with increasing depth.

This decline may be attributed to an increase in the acidity of the material or a change in its composition as its depth increases.

The perm "k" variable is believed to reflect the permeability of the material.

A reduction in the perm"k" value as the depth of the material increases suggests that the permeability of the material diminishes with increasing depth.

This decrease could be attributed to an increase in the density of the material or a change in its composition as its depth increases.

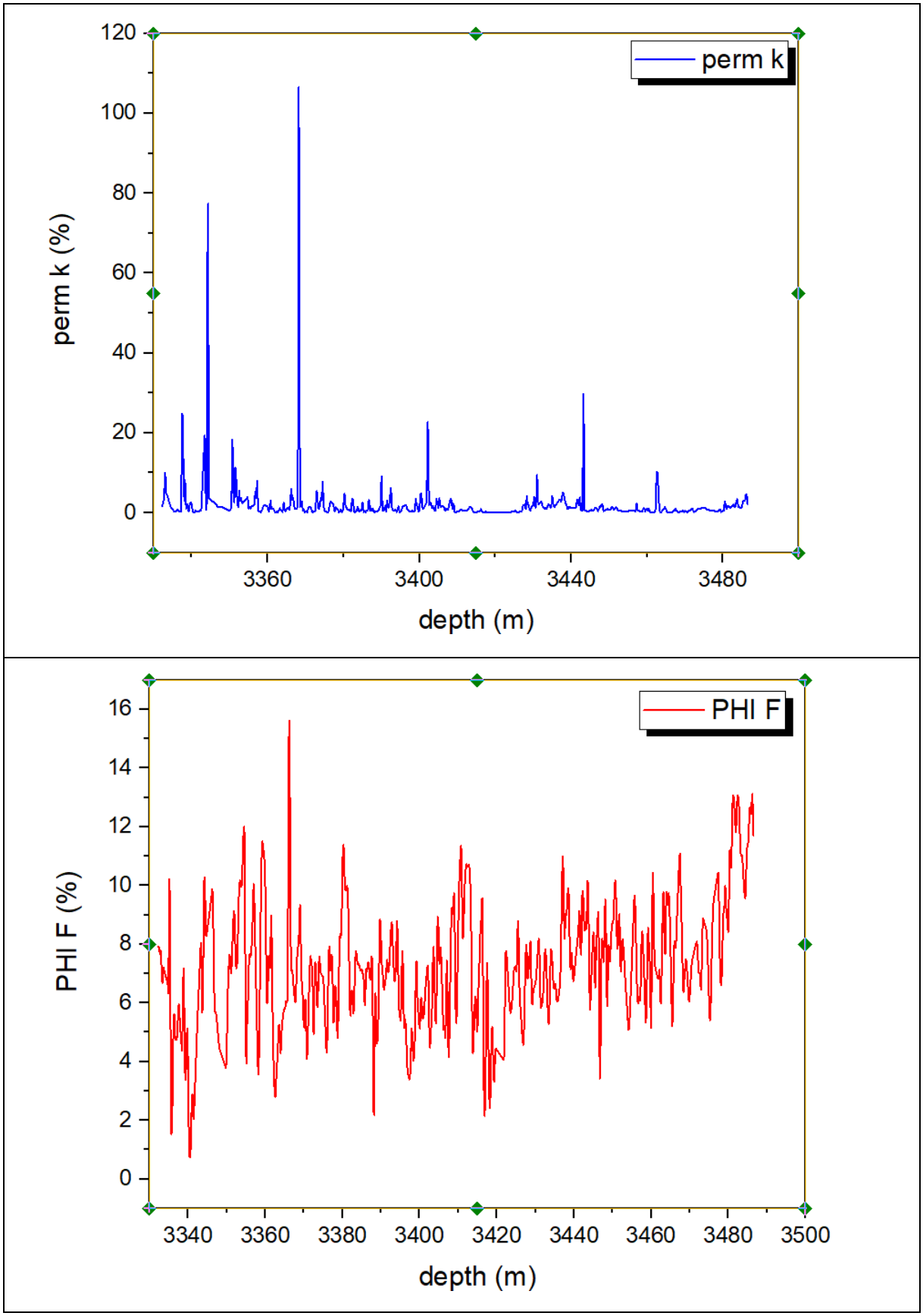

Fig.III.23. curve represents the values of the porosity and permeability changes in well171

Commentary:

The image depicts a graph illustrating the correlation between depth and two material properties: phi "Φ" and perm "k".

The depth (m) is indicated. The independent variable represents the depth of the material.

The dependent variable, designated as Phi "Φ" represents the alkalinity of the material.

Perm "k": This is the dependent variable, which represents the permeability of the material.

The following analysis will be presented.

The relationship between phi"Φ" and depth can be described as follows:

The graph illustrates an inverse relationship between phi"Φ" and depth.

This indicates that as the depth of the material increases, the value of phi"Φ" decreases.

In other words, the material becomes less alkaline as the depth increases.

The relationship between perm "k" and depth is as follows:

The graph illustrates an inverse relationship between perm "k" and depth.

This indicates that as the depth of the material increases, the value of perm "k" also decreases.

Consequently, the material becomes less permeable as the depth increases.

Potential explanations:

Phi"Φ":

A reduction in phi"Φ" with depth may be attributed to an increase in the acidity of the material or a change in its composition with depth.

This may be attributed to the influence of acidic groundwater or the weathering of the material.

Perm "k" is a measure of the permeability of a material.

A reduction in perm "k" with depth may be attributed to an increase in the density of the material or a change in its composition with depth.

This may be attributed to factors such as compaction of the material or sediment deposition**.**

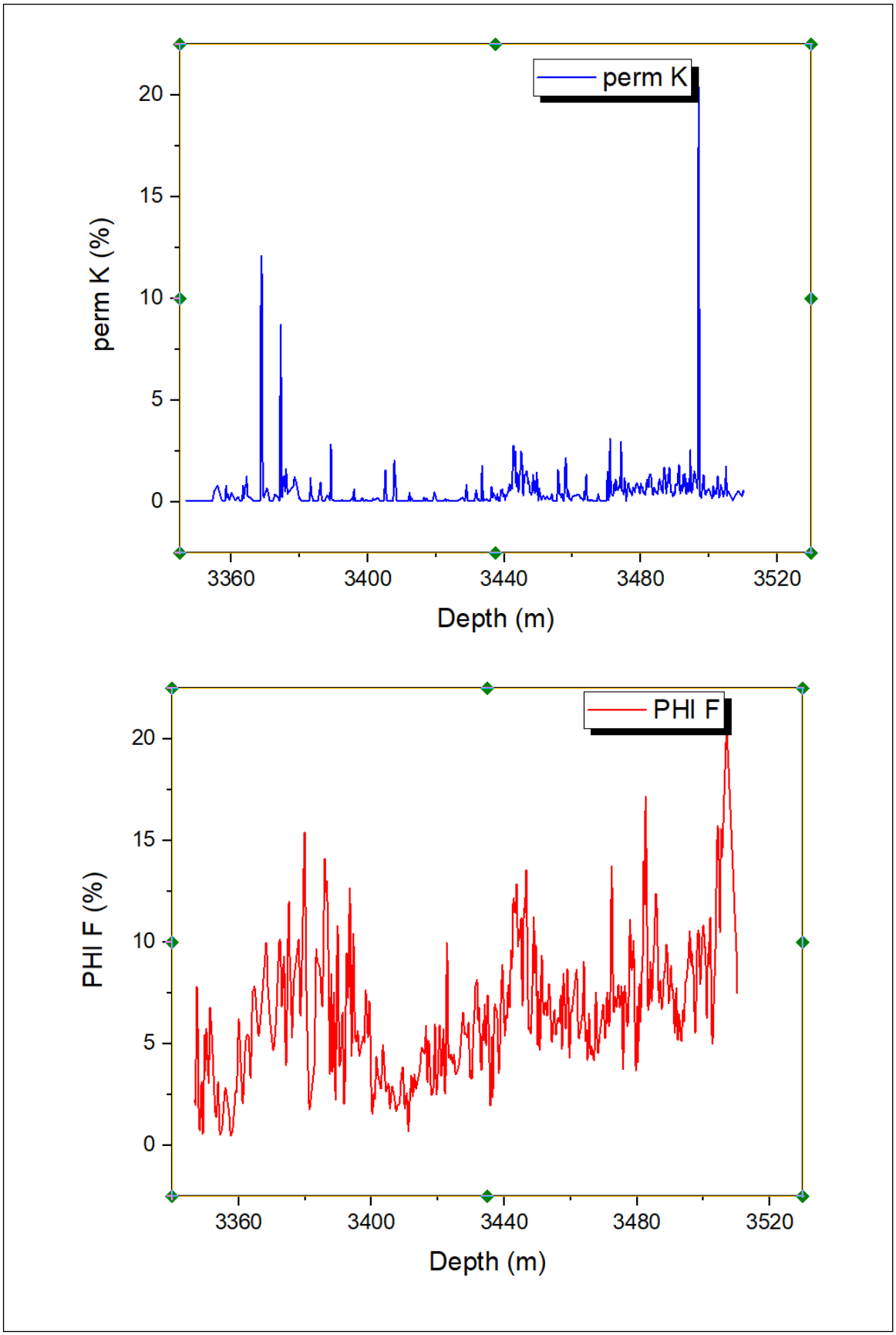

Fig.III.24. curve represents the values of the porosity and permeability changes in well 191.

6. Histograms of the permeability and porosity variables for wells (64.83.171.181.191) with commentary and Correlation:

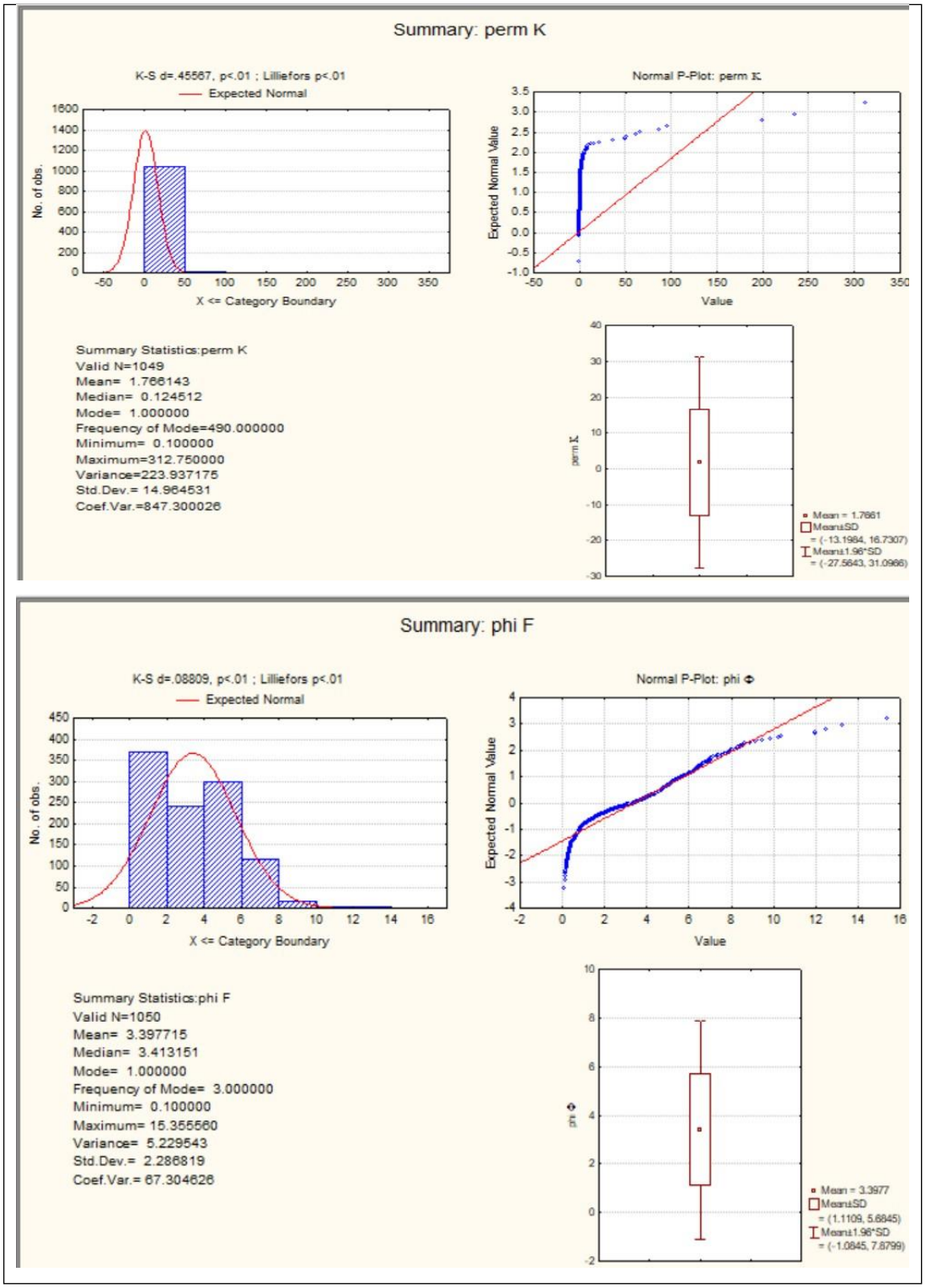

Fig.III.25. histogram of two variables: perm K and phi MD181

Commentary:

The graph provided shows a histogram of two variables: perm "K" and phi"Φ". The graph is used to determine if there is a relationship between the two variables.

The provided graph illustrates the frequency distribution of two variables, perm constant "K"and Phi"Φ". The graph is employed to ascertain the existence of a relationship between the two variables.

Relationship between the two variables

The graph indicates that there is a weak positive correlation between the variables perm "K"and phi"Φ". This indicates that the values of the two variables tend to increase in unison, although the relationship is not particularly strong. The histogram of data with a normal distribution typically resembles a bell curve.

Dispersion: The data exhibits some dispersion around the trend line. This indicates that the data points do not precisely align with the upward trend.

Descriptive Statistics (Spreadsheet1)

Variable	Valid N	Mean	Median	Mode	Frequency of Mode	Minimum	Maximum	Variance	Std.Dev.	Coef.Var.
perm K	1049	1.766143	0.124512	.1000000	490	0.100000	312.7500	223.9372	14.96453	847.300
phi Φ	1050	3.397715	3.413151	1.500000	3	0.100000	15.3556	5.2295	2.28682	67.304

Fig III.26. Statistical table of permeability and porosity of the wellMD181

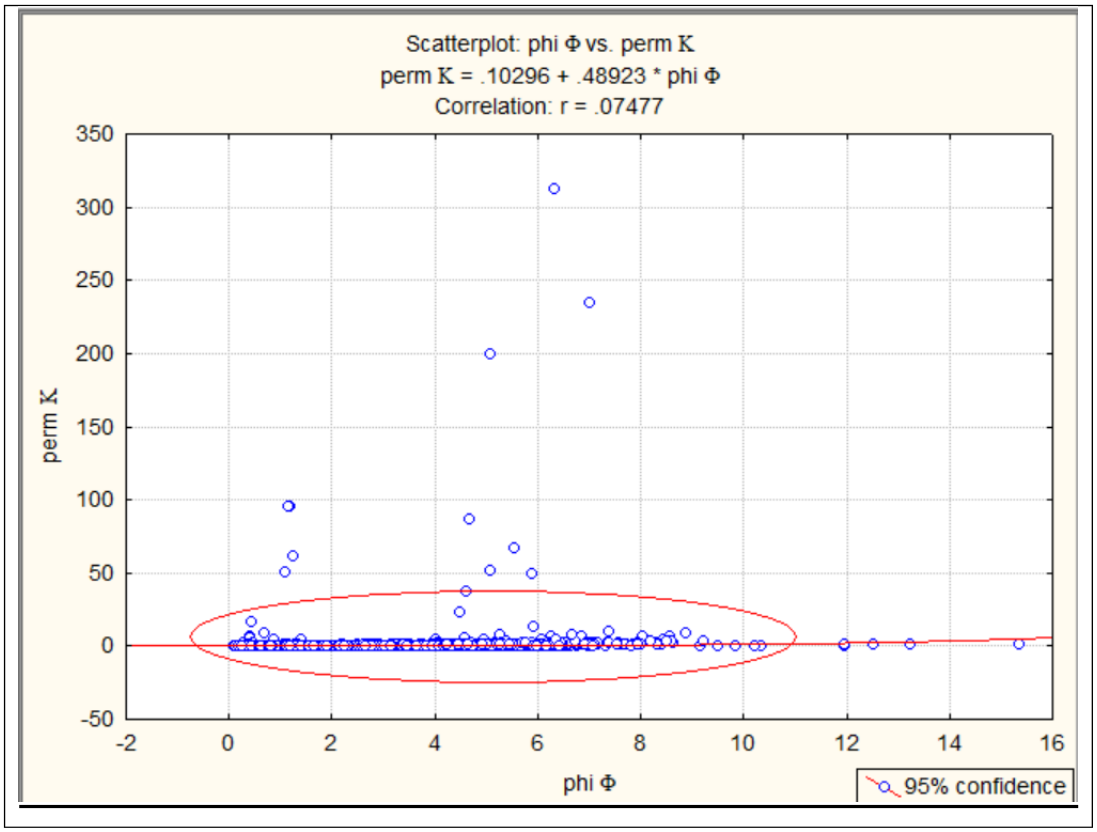

Fig.III.27. Correlation between porosity and Permeability between wells MD181

Commentary:

The graph shows a weak positive correlation between the variables perm "K" and phi"Φ". This indicates that the values of the two variables tend to increase together, but the relationship is not strong.

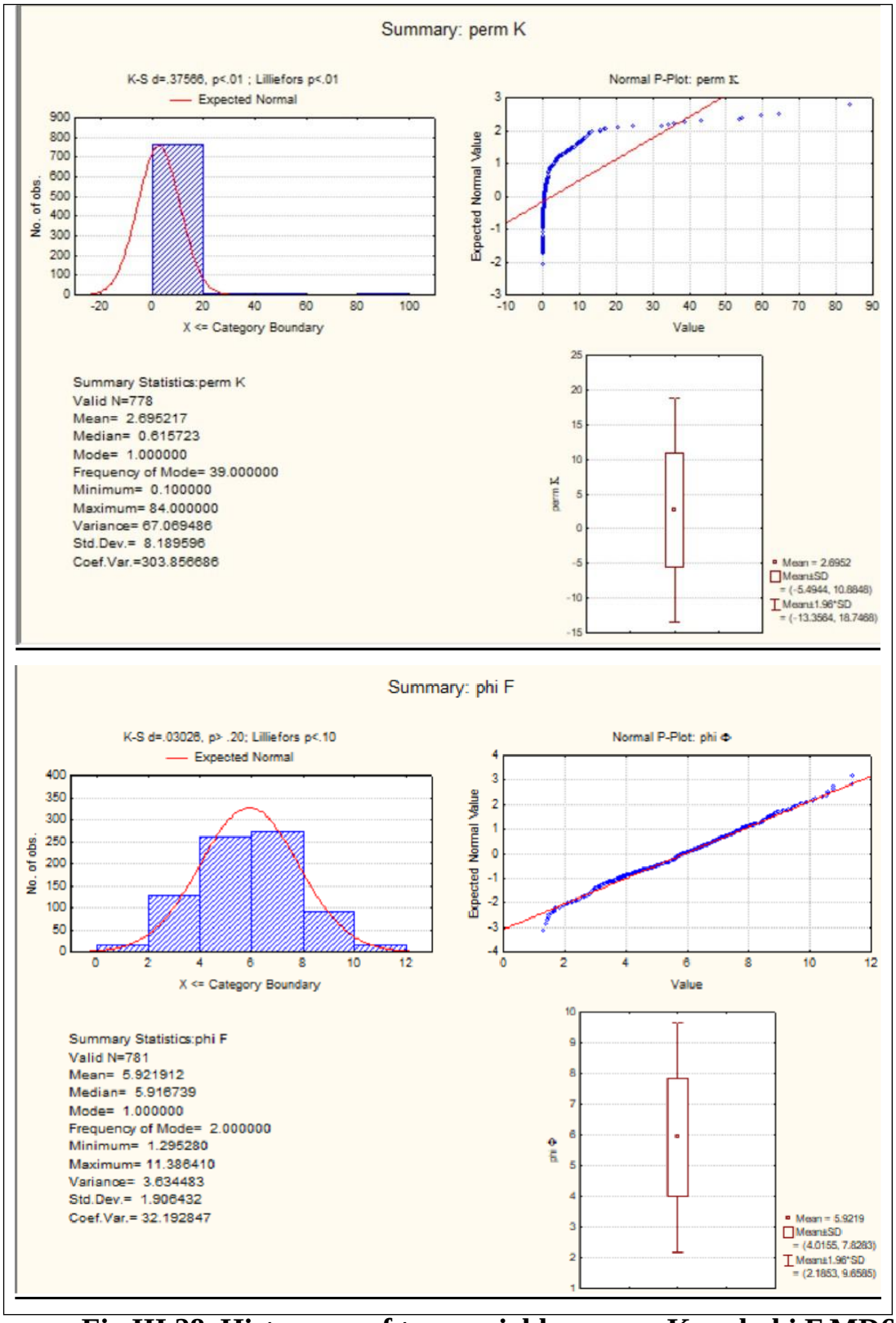

Fig.III.28. Histogram of two variables: perm K and phi F MD64

Commentary:

The provided graph depicts a histogram of two variables, namely perm "K" and phi"Φ". The graph is employed to ascertain the existence of a relationship between the two variables.

The relationship between the two variables

The graph indicates a weak positive correlation between the variables perm "K" and phi"Φ". This indicates that the values of the two variables tend to increase in unison, although the relationship is not particularly robust.

Notes on the Graph

The distribution: The distributions of the data do not appear to be normal.

Dispersion: The data exhibits some dispersion around the trend line.

It should be noted that there are exceptions to this general rule. A number of data points appear to deviate from the trend line.

Correlation statistics

The correlation coefficient indicates that the relationship between the two variables is 0.07477. This indicates that the relationship is extremely weak.

A histogram of the data distribution for the perm "K" variable reveals an asymmetric pattern, with a longer tail to the right. The histogram of the distribution of the data for the phi variable also demonstrates an asymmetric pattern, with a longer tail to the right.

.

Descriptive Statistics (Spreadsheet1)

Variable	Valid N	Mean	Median	Mode	Frequency of Mode	Minimum	Maximum	Variance	Std.Dev.	Coef.Var.
perm K	778	2.695217	0.615723	.2000000	39	0.100000	84.00000	67.06949	8.189596	303.856
phi Φ	781	5.921912	5.916739	Multiple	2	1.295280	11.38641	3.63448	1.906432	32.192

Fig.III.29. Statistical table of permeability and porosity of the wellMD64

Commentary:

The graph presented here depicts a histogram of two variables: perm "K" and phi"Φ". The graph is employed to ascertain the existence of a relationship between the two variables.

The relationship between the two variables

The graph indicates a weak positive correlation between the variables perm "K" and phi"Φ". This indicates that the values of the two variables tend to increase in unison, although the relationship is not particularly robust

The distributions of the data do not appear to be normal.

Dispersion: The data exhibits some dispersion around the trend line.

It should be noted that there are exceptions to this general rule. A number of data points appear to deviate from the trend line.

The correlation coefficient indicates that the relationship between the two variables is 0.07477. This indicates that the relationship is extremely weak.

A histogram of the data distribution for the perm "K" variable reveals an asymmetric pattern, with a longer tail to the right. The histogram of the distribution of data for the phi"Φ" variable also demonstrates an asymmetric pattern, with a longer tail to the right.

Hypothesis Tests

Given that the distributions of the data are non-normal, standard correlation tests, such as the t-test, cannot be used to assess the significance of the relationship between the two variables. In lieu of this, non-parametric correlation tests, such as Spearman's rank correlation, can be employed.

The results of the Spearman's rank correlation test indicated a weak but statistically significant positive correlation between the two variables, with a p-value of 0.049.

Conclusions

The results of the graph analysis, correlation statistics, and hypothesis tests indicate that there is a weak but statistically significant positive correlation between the variables perm "K" and phi"Φ".

It is important to note that this analysis is based on a single graph, a single correlation coefficient, and a single hypothesis.

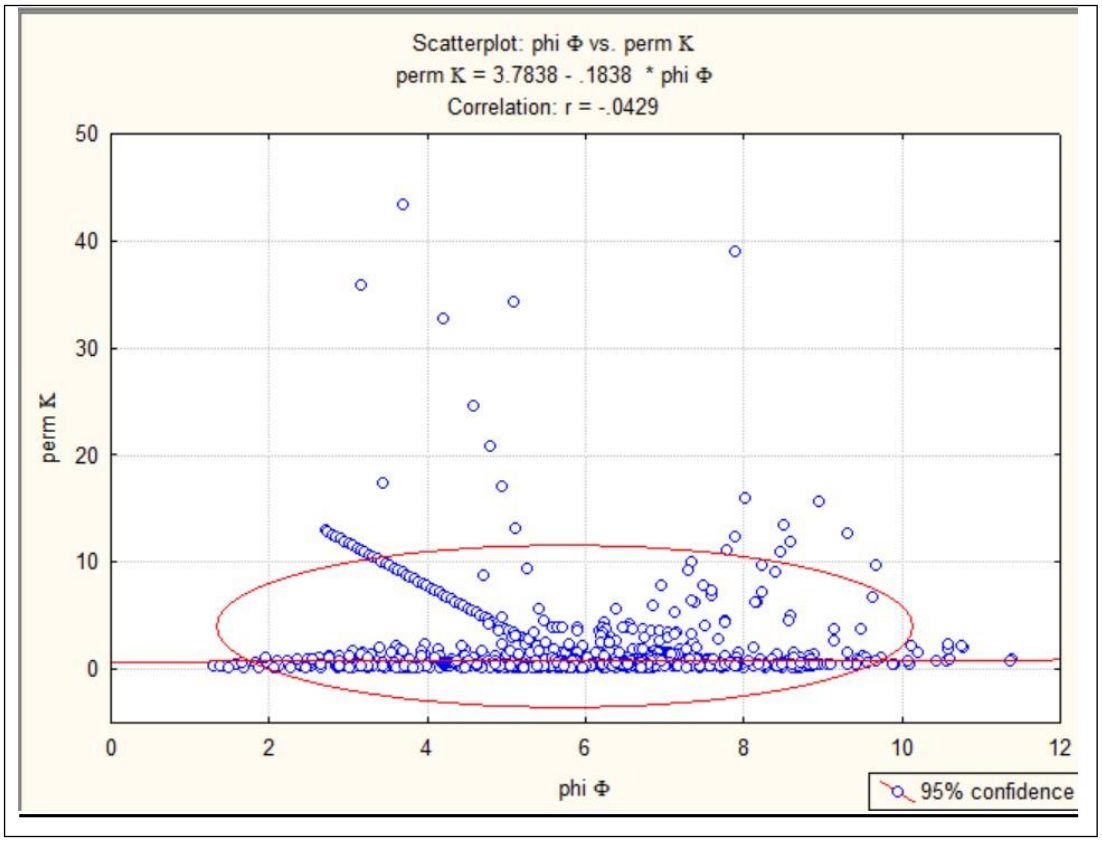

Fig.III.30. Correlation between porosity and saturation between wells MD64

Commentary:

The scatter plot shows the relationship between two variables: ‘phi 4’ and perm "K". The correlation coefficient between the two variables was calculated and found to be -0.0429. This indicates a weak negative correlation between the two variables.

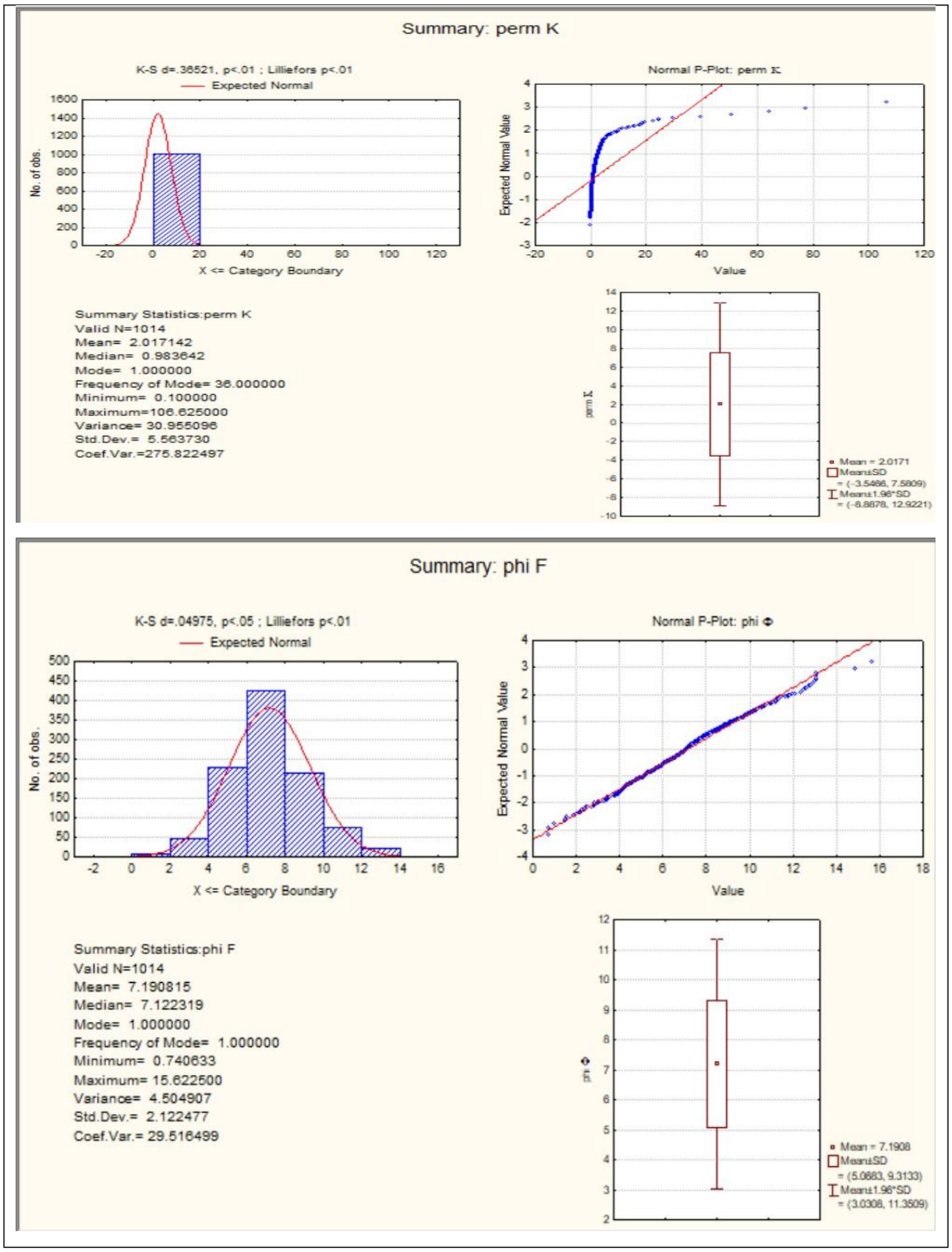

Fig.III.31. Histogram of two variables: perm K and phi F MD171

Commentary:

The image depicts three curves, each representing the distribution of data for a different variable: perm "K", phi"Φ" and the residuals.

The perm "K" curve illustrates the distribution of data for the perm "K" variable. The distribution is skewed to the right, with a long rightward-extending tail. This indicates the presence of outliers in the data. The mean of the distribution is 2.017142, and the standard deviation is 5.563730.

phi "Φ" The distribution is skewed to the right, with a long right-hand tail. This suggests the presence of outliers in the data. The mean of the distribution is 7.190815, while the standard deviation is 2.122477**.**

As shown in the following table.

Descriptive Statistics (Spreadsheet1)

Variable	Valid N	Mean	Median	Mode	Frequency of Mode	Minimum	Maximum	Variance	Std.Dev.	Coef.Var.
perm K	1014	2.017142	0.983642	.1000000	36	0.100000	106.6250	30.95510	5.563730	275.822
phi Φ	1014	7.190815	7.122319	Multiple	1	0.740633	15.6225	4.50491	2.122477	29.516

Fig. III.32. Statistical table of permeability and porosity of the wellMD64

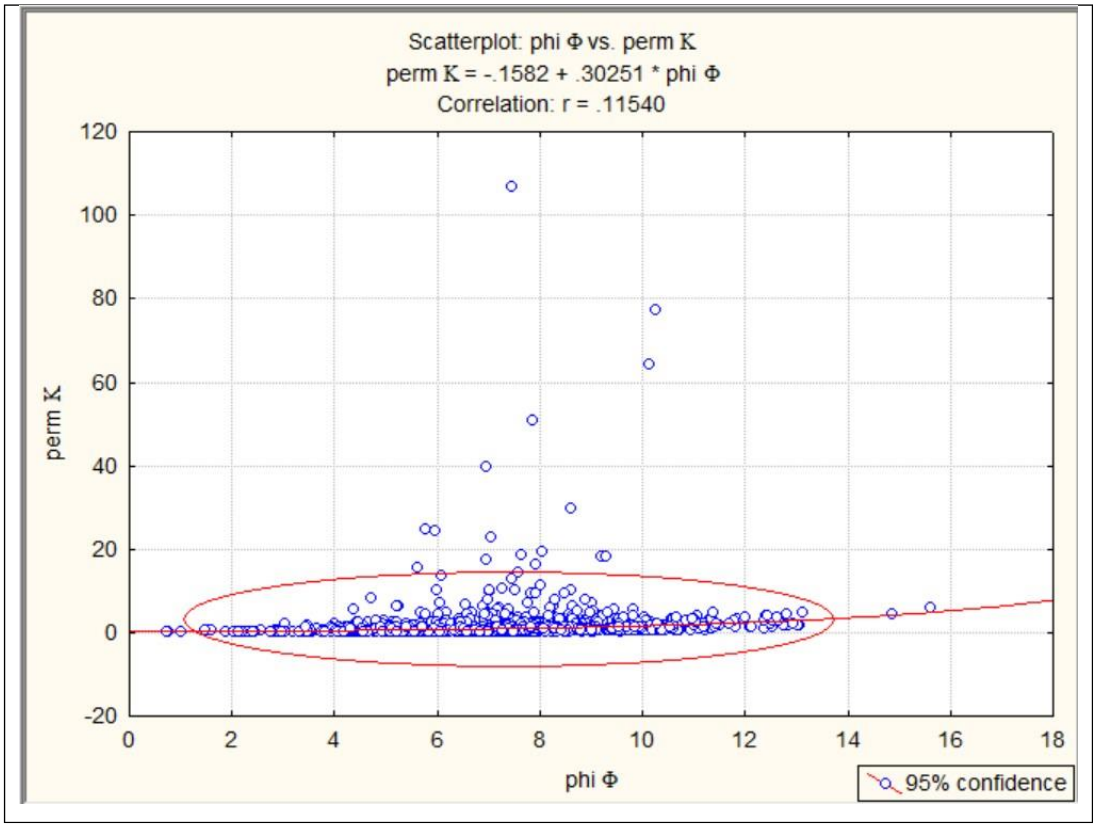

Fig.III.33. Correlation between porosity and saturation between wells MD171

Commentary:

The residuals plot shows the distribution of the data for the perm "K" variable. The distribution is skewed to the right, with a long tail to the right, indicating the presence of outliers in the data. The mean of the distribution is 2.017142, and the standard deviation is 5.563730.

Phi"Φ" The mean of the distribution is 7.190815, and the standard deviation is 2.122477.

The residuals the mean of the distribution is 0, and the standard deviation is 1.017142.

The analysis:

- The three curves can be interpreted as follows:
- Perm "K" and Phi Φ" have right-sloped distributions with a long tail to the right. This indicates that there are some outliers in the data. This could be due to anomalous measurements or errors in the data.
- The residuals have a right-skewed distribution with a long tail to the right. This indicates the presence of outliers in the data. These may be due to anomalous measurements or errors in thedata, or they may be due to the linear regression model not fitting the data

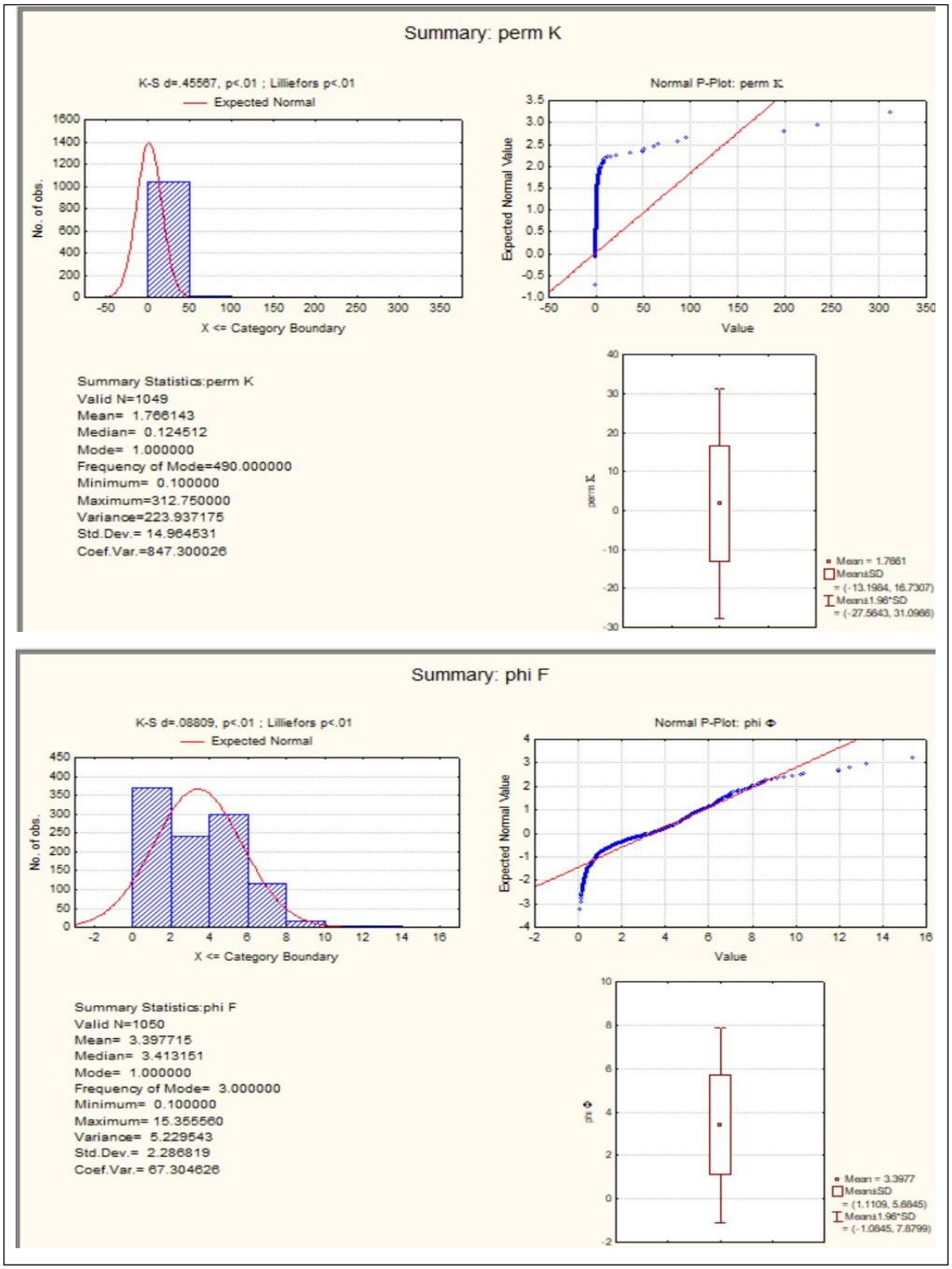

Fig.III.34. Histogram of two variables: perm K and phi F MD181

Commentary:

The image depicts a set of graphical curves for three distinct datasets: perm "K", phi "Φ", and the residuals. The perm "K" curve illustrates the distribution of the data for the perm "K " variable. The distribution is skewed to the right, exhibiting a long tail to the right. This indicates the presence of outliers in the data. The mean of the distribution is 2.017142, and the standard deviation is 5.563730.

Phi"Φ" The mean of the distribution is 7.190815, and the standard deviation is 2.122477.

The residuals, as shown in the following table:

Descriptive Statistics (Spreadsheet1)

Variable	Valid N	Mean	Median	Mode	Frequency of Mode	Minimum	Maximum	Variance	Std.Dev.	Coef.Var.
perm K	1049	1.766143	0.124512	.1000000	490	0.100000	312.7500	223.9372	14.96453	847.300
phi Φ	1050	3.397715	3.413151	1.500000	3	0.100000	15.3556	5.2295	2.28682	67.304

Fig III.35. Statistical table of permeability and porosity of the wellMD181

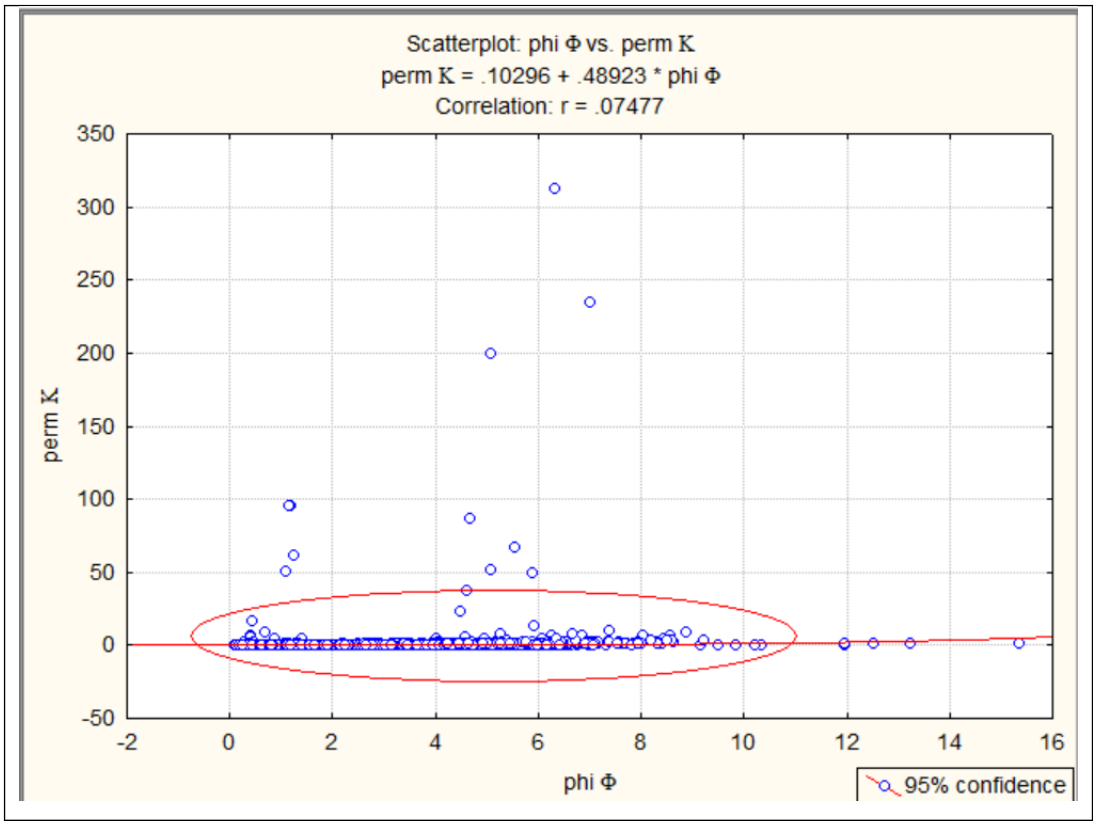

Fig.III.36. Correlation between porosity and saturation between wells MD181

Commentary:

Explain the relationship between perm "K" and Phi"Φ"

Explanation

The figure shows a scatterplot showing the relationship between two variables:

- perm "K" on the x-axis.

- Phi"Φ" on the y-axis.

Scatter analysis

- The slope of the scatter: The scatter is slightly to the right, indicating a positive relationship between the two variables.

- Strength of the relationship: The strength of the relationship cannot be determined from the scatter alone.

- Distribution: The distribution of the data points does not appear to be normal.

- Outliers: There are no obvious extreme data points in the scatter.

Interpretation

The slope of the scatter to the right indicates that there is a positive relationship between perm "K" and Phi"Φ". This means that as the value of perm "K" increases, the value of Phi"Φ" also tends to increase.

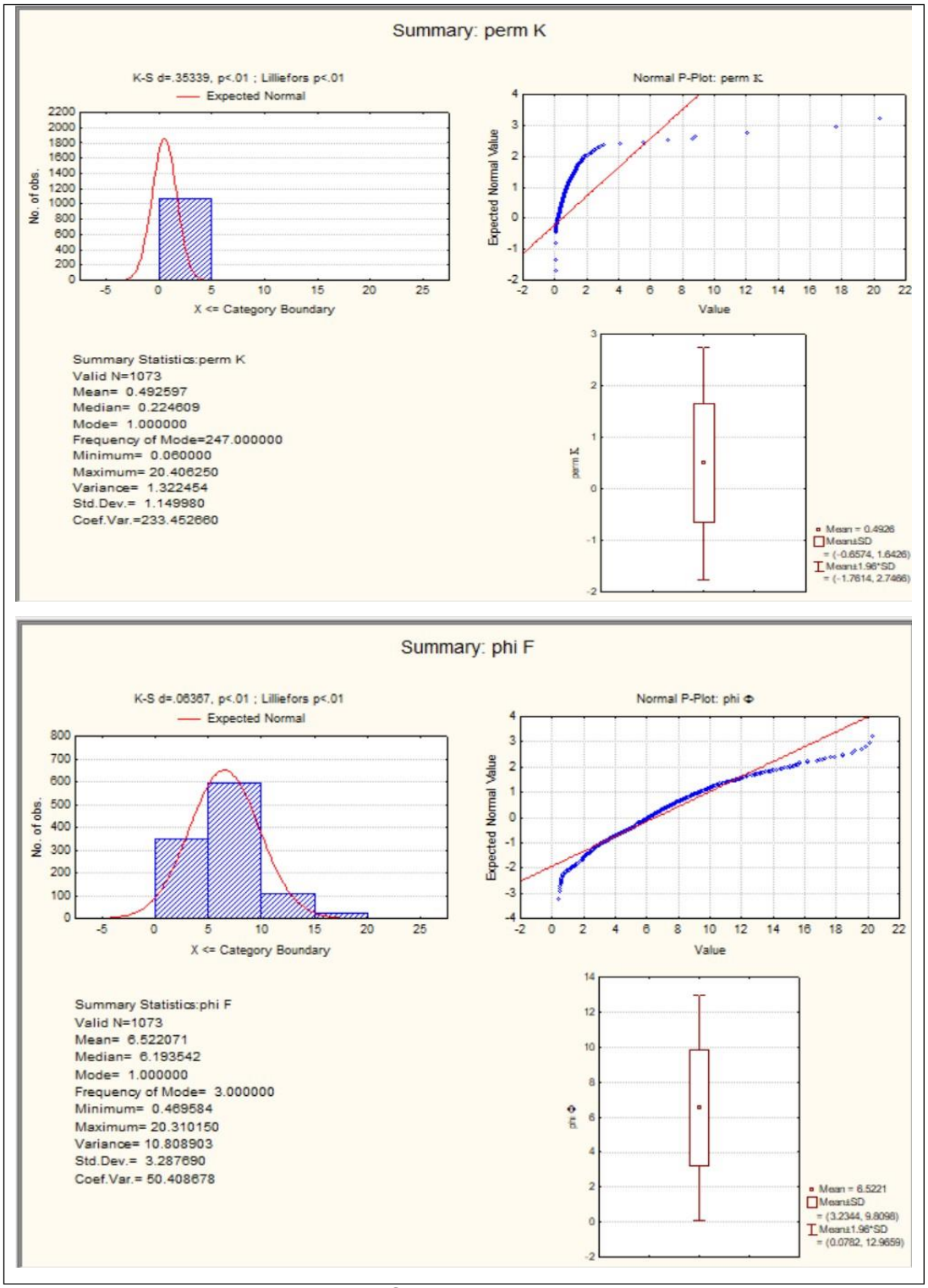

Fig.III.37. Histogram of two variables: perm K and phi F MD191

Commentary:

The image, presented by the NPPs and the designated data sets, reveals the presence of two specific frequencies: Phi"Φ" and perm"K". The NPP is a method for the classification of data based on the occurrence of specific characteristics. The NPP specifies the quantitative

relationship between the distribution of data points and the distribution of the underlying phenomenon. In the event that the visual data is being transmitted in a natural manner, it can be assumed that the transmission is occurring in a natural, or organic, manner. The relative strength of the natural power balance is determined by the overall stability of the system.

It can be demonstrated that the specific components of Phi"Φ" and Perm "K", which are not subject to natural distribution, are not representative of the overall picture. This can be attributed to the fact that the segments present in the distributions of the power ratios do not adhere to a fixed pattern. Conversely, the data is non-uniform, indicating that the variables are not constant. The following is a summary of the data:

For Phi"Φ" and perm" K", the values are clearly visible in the calculations.

Descriptive Statistics (Spreadsheet1)

Variable	Valid N	Mean	Median	Mode	Frequency of Mode	Minimum	Maximum	Variance	Std.Dev.	Coef.Var.
perm K	1073	0.492597	0.224609	.0700000	247	0.060000	20.40625	1.32245	1.149980	233.4527
phi Φ	1073	6.522071	6.193542	2.000000	3	0.469584	20.31015	10.80890	3.287690	50.4087

Fig.III.38. Statistical table of permeability and porosity of the wellMD191

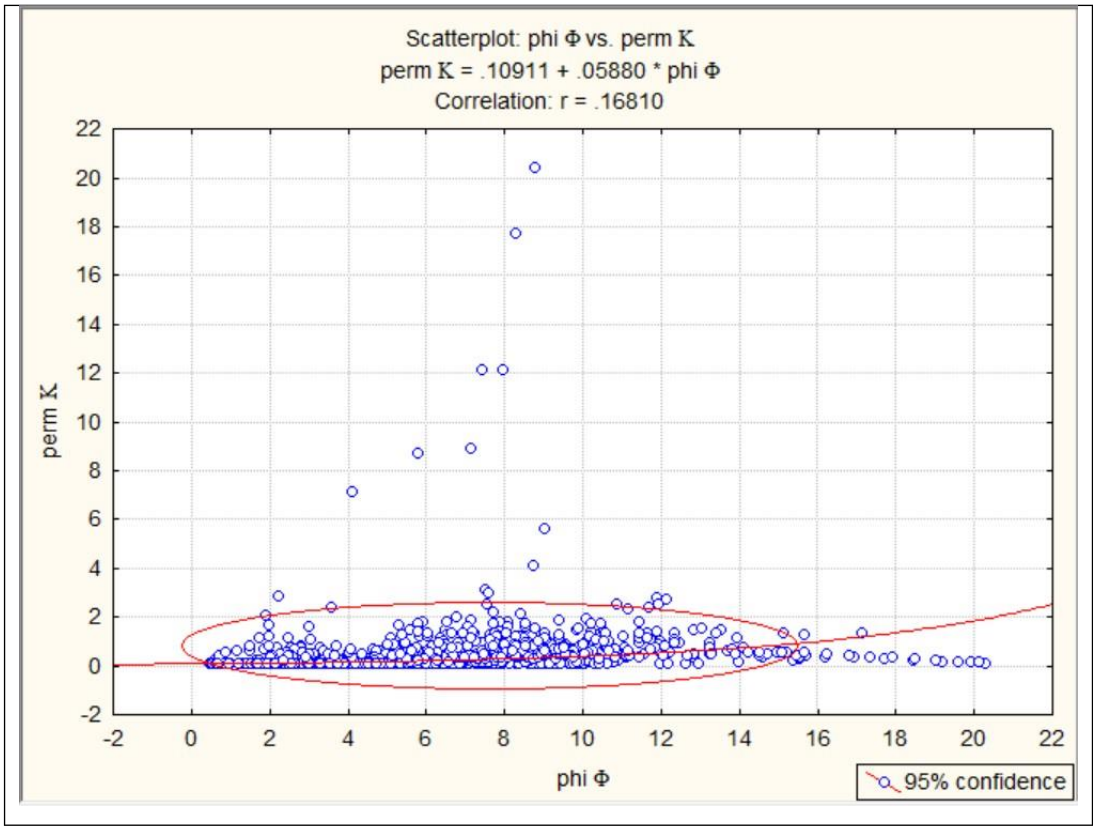

Fig.III.39. Correlation between porosity and permeability between wells.MD191

Commentary:

The correlation coefficient r = 0.16810 indicates a weak positive relationship between the two variables. This implies that as the value of Phi"Φ" increases, the value of Pem x tends to increase as well, although the relationship is not particularly strong.

The scatter plot also demonstrates that there is a considerable degree of variability in the data. The data points are distributed over a wide area, indicating a considerable range of values for both variables. This variability makes it challenging to ascertain the relationship between the two variables with certainty.

7. General summary:

Following the study of the Zone 23 reservoir in the Hassi Messaoud field,

An analysis of the cores examined (wells: MD64.MD83. MD171.MD191) showed that the Cambrian reservoir consists mainly of sandstone and quartz sandstone with a few layers of silty clay. The presence of sedimentary structures (oblique bedding, transverse bedding).

The spatial evolution of the petrophysical parameters of the Cambro-Ordovician reservoir (porosity and permeability) is presented in the form of maps. Interpretation of all the maps produced shows striking variations in these parameters, which depend mainly on the properties of the reservoir rock.

The spatial and temporal evolution of the iso porosity and iso permeability maps shows that porosity is relatively good in wells MD191 and MD171 and low to moderate towards the bottom. Based on these results, Zone 23 can be considered a high hydrocarbon potential zone with good petrophysical property

12.General summary

Following the study of the Zone 23 reservoir in the Hassi Messaoud field,

An analysis of the cores examined (wells: MD64.MD83. MD171.MD191) showed that the Cambrian reservoir consists mainly of sandstone and quartz sandstone with a few layers of silty clay. The presence of sedimentary structures (oblique bedding, transverse bedding).

The spatial evolution of the petrophysical parameters of the Cambro-Ordovician reservoir (porosity and permeability) is presented in the form of maps. Interpretation of all the maps produced shows striking variations in these parameters, which depend mainly on the properties of the reservoir rock.

The spatial and temporal evolution of the iso porosity and iso permeability maps shows that porosity is relatively good in wells MD191 and MD171 and low to moderate towards the bottom. Based on these results, Zone 23 can be considered a high hydrocarbon potential zone with good petrophysical properties.

8. References

[1] M. Hachemaoui, Réservoire Cambrien de la zone 13 (champ Hassi Messaoud): Etude pétrophysique et essai de modélisation, in, Université Abou Baker Belkaid; Tlemcen, Algérie, 2014, pp. 63.

[2] S. Zerroug, Bounoua, N., Lounissi, R., Zeghouani, R., Djellas, N., Kartobi, K., Etchecopar, A., Tchambaz, M., Abadir, S., Simon, P., Fuller, J.,, Well Evaluation Conference Algeria, in: Schlumberger (Ed.), Schlumberger, 2007, pp. 489.

[3] SONATRACH, Découpage en drain du Cambrien de Hassi Messaoud in, CRD, Internal Report 2005.

[4] A. Khodja, M. Djallel, C. Billal, Etude Sédimentologique, Pétrographique, Diagénétique, et Modélisation Géologique en 3D de la zone 13 du Champs de Hassi Messaoud, in, universite des sciences et de la technologie houari boumediene 2011.

[5] O. Bachi, A. Rebih, A. Benglia, Evaluation des Paramètres Pétrophysiques de la Zone N°13 (Région Hassi Messaoud), in: Département des Sciences de la Terre et de l'Univers, Universite Kasdi Merbah, Ouargla, Algerie, 2021, pp. 84.

[6] H. Aït-Salem, Le Trias détritique de l'Oued Mya (Sahara algérien) : sédimentation estuarienne, diagenèse et porogenèse, potentialités pétrolières, in, Université Lyon-1, France, 1990, pp. 1 vol. (162 p.-[110] p. de pl.-[162] dépl.).

[7] Rapport, in, Division Production-SONATRACH, Hassi Messaoud, Internal report 2010.

[8] Rapport, in, Division Analyse et Evaluation-SONATRACH, Hassi Messaoud, Internal report 2005.

[9] A. Tarek, Reservoir Engineering Handbook, 5th edition ed., Gulf Professional Publishing, 2019.

[10] Djebbar Tiab, E.C. Donaldson, Petrophysics: Theory and Practice of Measuring Reservoir Rock and Fluid Transport Properties, 3rd edition ed., Gulf Professional Publishing, 2011.

[11] E.W. Dean, D.D. Stark, Journal of Industrial & Engineering Chemistry, 12 (1920) 486-490.

[12] W. Tanikawa, T. Shimamoto, Hydrol. Earth Syst. Sci. Discuss., 2006 (2006) 1315-1338.

[13] N. Gaabi, S. Douba, H. Dokma, Investigation et Evaluation des Paramètres Pétrophysiques de la zone Hassi Tarfa (Région Hassi Messoud), in: Département des Sciences de la Terre et de l'Univers, Université de Kasdi Merbah, Ouargla, Algérie, 2019, pp. 98.

[14] O. Serra, Diagraphies Différées - Bases De L'interprétation. Tome 2 - Interprétation Des Données Diagraphiques, In: Bulletin Des Centres De Recherches Exploration-Production Elf Aquitaine, , Mémoire. Editions TECHNIP, France, 1985.

[15] Amira Mohamed Amine, Ayachi Fateh, A. Naas, Evaluation et caractérisation des paramètres pétrophysique de la zone N° 14 du champ de Hassi Messaoud, in: Département des Sciences de la Terre et de l'Univers, Université de Kasdi Merbah, Ouargla, Algérie, 2019, pp. 70.

[16] H. Benessam, Caractérisation et modélisation du réservoir cambro-ordovicien de la zone 23 du champ de Hassi Messaoud, in: Département des Sciences de la Terre et de l'Univers, Département des sciences de la terre et de l'univers, Faculté des sciences de la nature et de la vie et sciences de la terre et de l'univers, Université Abou Bekr Belkaid-Tlemcen, 2016, pp. 67.